Evaluation of Soft Switching for EV and HEV Motor Drives

Mehrdad Ehsani, *Fellow, IEEE*
Khwaja M. Rahman, *Student Member, IEEE*
Maria D. Bellar, *Student Member, IEEE*
Alex Severinsky, *Senior Member, IEEE*

Texas A&M University
Department of Electrical Engineering
College Station, TX 77843-3128
Phone: (409) 845-7582
Fax: (409) 862-1976

***Abstract*-Soft switching has the potential of reducing switch stresses and of lowering the switching losses as compared to hard switching. For this reason, several soft switching topologies have been presented in the literature. Each topology has some advantages. Their operation, however, requires additional active and/or passive elements. This introduces additional cost and complexity. To understand the effectiveness of the soft switching technique, when applied to electric vehicle (EV) and hybrid electric vehicle (HEV) systems, it may be necessary to first evaluate their system requirements and performances. This evaluation process would require knowledge of the vehicle dynamics. The vehicle load requires a special torque-speed profile from the drive train for minimum power ratings to meet the vehicle's operational constraints such as, initial acceleration and gradability. The selection of motor and its control for EV and HEV applications is dictated mainly by this special torque-speed requirement. As a consequence, this requirement will have a strong influence on the converter operation. This paper makes an attempt to evaluate EV and HEV running in both standard FTP75 city driving cycle and highway driving cycle. The analysis will be carried out for several most commonly used electric motors operating on the optimal torque-speed profile. Special attention will be given to the converter losses. Features of the soft switching will be evaluated in the context of the dynamic vehicle power flow and the system losses, as well as the power converter requirements. The relative significance of soft switching for EV and HEV systems will then be established.**

I. Introduction

Power switches are an integral part of any power converter circuit. Unfortunately, they are also the major source of power dissipation in the circuit. This power dissipation is caused by two features. One is conduction voltage drop in the switch while the switch is conducting. Some devices have lower conduction drops (MCT, BJT), hence lower conduction losses, while other devices have medium to high conduction drops (IGBT, MOSFET), hence medium to high conduction losses. The other cause of energy dissipation in a power switch is the dynamics of the switching. Switching of current in the presence of a switch voltage and vice versa, commonly referred to as hard switching, causes power losses in the switch. The switching loss increases with the switching frequency. To reduce the switching loss very fast devices are built. These devices have very fast turn-on and turn-off characteristics. However, high di/dt and dv/dt associated with this fast switching increase stresses on the switch and causes EMI. To alleviate the difficulties associated with hard switching, the concept of soft switching was introduced. The main underlying principle in soft switching is to switch the power device at the instant when the switch current is zero, known as zero current switching (ZCS), or switch the device when switch voltage is zero, known as zero voltage switching (ZVS). This way both the switching loss and switch stresses can be reduced. Many soft-switched converter topologies have been presented in the literature [1-6]. The followings are usually claimed with respect to the operations of the soft-switched converter topologies:

- higher efficiency,
- better device utilization,
- reduced size of filtering elements,
- higher power density,
- reduced acoustic noise,
- reduced EMI,
- fast dynamic response,
- reduced torque and current ripple.

However, the operation of the soft-switched converters requires additional active and/or passive elements. This introduces additional cost and complexity. Moreover, some of the advantages listed above may be questionable and some may not be very critical for some applications. Therefore, it may be necessary to assess the effectiveness of soft switching compared to hard switching, in connection to specific applications. This paper, therefore, makes an attempt to evaluate soft switching for electric vehicle (EV) and hybrid electric vehicle (HEV) drivetrain applications. This evaluation is based on the systems performance and on the power converter requirements. First knowledge of the vehicle dynamics will be needed. A study of vehicle dynamics reveals that, the vehicle powertrain is required to exhibit a special torque-speed profile for minimizing the power requirement to meet the vehicle's operational constraints [7]. The selection of the electric motor and its control will be governed by this special torque-speed requirement. As a consequence, the converter operation will be greatly influenced by this special requirement. A simplified analysis is carried out on a system level for induction motor, switched reluctance motor (SRM), and brushless dc (BLDC) motor operating on the optimal

torque-speed profile. Efficiency is a maior issue, especially for EV operations. Hence, special attention will be given to the converter losses, as a means to evaluate the improvement in the system efficiency that could be achieved by using soft switching. The loss estimation will be carried out for the vehicle running in both standard FTP75 city driving cycle and highway driving cycle. The relative significance of soft switching for EV and HEV systems will then be established.

II. EV and HEV Characteristics

A. EV and HEV Architecture

Electric vehicles (EVs) use an electric motor for propulsion and battery as the only source of energy. These vehicles constitute the only commonly known group of automobiles that are classified as Zero Emission Vehicles (ZEVs). However, EVs suffer from range limitations. As a consequence, efficiency is a major issue for EV, since it relates directly to the range of the vehicle.

Hybrid electric vehicles (HEVs) are classified as Ultra Low Emission Vehicles (ULEVs), and do not suffer from the range limitations imposed on the EVs. This is due to the fact that the power train combines more than one energy source to propel the vehicle. There are many different power train configurations for hybrids, but in general, they fall into two categories: series and parallel. In series hybrid the ICE engine is normally used to charge a battery pack through a generator, while the electric motor propels the vehicle powered by the battery. It is also possible to direct the ICE power directly to the wheels through the motor generator pair when the battery is fully charged. Thus, the engine can be decoupled from the wheel and always run in the optimal efficiency region. However, the several stages of energy conversions have their associated power losses. In contrast, the parallel hybrid system connects both the ICE and the electric motor in parallel. These two components directly provide the power into the wheel.

In series hybrid system, the electric motor behaves exactly in the same manner as in an electric vehicle. Therefore, the torque and power requirements of the electric motor are roughly equal for an EV and series hybrid, while they are comparatively lower for parallel hybrid. For HEVs, electrical efficiency is not as critical as it is in the case of EVs.

B. Optimal Torque Speed Profile for EV and HEV Drivetrain

Our recent study has shown that, a vehicle, can meet its performance requirements with minimum power rating if the powertrain operates mostly in constant power [7]. The power rating of a motor that deviates from the constant power regime can be as much as two times that of a motor operating at constant power throughout its speed range in a vehicle.

The electric motor in its normal mode of operation can provide constant rated torque up to its base or rated speed. At this speed, the motor reaches its rated power limit. The operation beyond the base speed, up to the maximum speed, is limited to this constant power region. The range of this constant power operation depends primarily on the particular motor type and its control strategy. It is obvious from the previous discussion that an electric machine must be capable of performing a long constant power operation in order to be suitable for EV and HEV applications. A range of six times the base speed in constant power would generally be required in order to reduce the power requirement to an appreciable level [7]. Clearly, for normal vehicle operation the optimal motor will operate mainly in constant power range. In our study, therefore, special attention will be given to the converter operation for high speed constant power operation of the drivetrain.

The specification of the power of the motor along with its power factor (pf) of operation will define the VA rating of the converter. Since different types of motors have different constant power capabilities and have different pf of operation, the converter VA rating will be different for each motor.

C. Methods of Torque Control at Low Speed and High Speed

The method of torque control below base speed, when the back emf is lower than the DC bus voltage, is similar for all motors. It usually involves PWM chopping of the current for the control of the torque. However, the torque control method above base speed, when the back emf exceeds the bus voltage, is motor and control dependent.

In the case of the induction motor, the usual practice is to begin field weakening once the motor speed exceeds the base speed. This way, the back emf is not allowed to build up beyond the bus voltage. Nevertheless, in order to retain the PWM current control capability at high speed, the electric motor would need to enter the field weakening before reaching the base speed. This would, however, reduce the available torque at high speed. To maximize the torque capability at high speed, six-step mode of operation seems to be inevitable because of the limited bus voltage [8]. Torque control in this mode and smooth transition between current regulated PWM mode and six-step mode becomes an important issue.

SRM is a singly fed motor as is the induction motor. Both the excitation current and the torque current are fed through the stator. However, unlike the induction motor, no control method is known that can isolate the torque component of current from the field component of current. Hence, field weakening is not possible in the SRM. Operation in constant power is made possible in this motor by the phase advancing of the stator current conduction angle until overlapping between the successive phases occurs [9]. Due to the high back emf, which cannot be weakened, PWM control of current is not possible in the extended speed range of operation.

Operation of the BLDC motor in the extended speed constant power range is similar to SRM. Due to the presence of the permanent magnet field which can only be weakened through a production of a stator field component which opposes the rotor magnetic field, field weakening is difficult in BLDC motor. Extended constant power operation is possible through the advancing of the commutation angle [10-12].

In summary we conclude that the switching of the DC bus by the converter is dictated by the torque control method. That is, the torque at low speed will be controlled by the PWM

control of the current. However, to maximize the torque capability of electric motor drives for EV and HEV applications, torque at high speed will be controlled by controlling the phase of the input voltage (phase-shift control). Since the control operation influences the number of switchings performed by the converter, it will influence the switching losses. Hence, torque control scheme of each motor will be studied in detail in this paper in an attempt to estimate the switching losses for EV and HEV application.

III. EV and HEV Drivetrain Model Considerations

In this section, some vehicle characteristics, motor and power converter considerations for modeling EV and HEV drivetrains are presented. The main objective is to calculate the converter switching and conduction losses for both systems. Also, the use of induction motor (IM), brushless dc (BLDC) motor and switched reluctance motor (SRM) is considered in the study of the two systems.

The vehicle characteristics of a typical 4-seat passenger car are given below:

- 0-26.82 m/s (0-60 mph) in 10 seconds.
- vehicle mass of 1700 kg.
- rolling resistance coefficient of 0.013.
- aerodynamic drag coefficient of 0.29.
- wheel radius of 0.2794 m (11 inch).
- level ground.
- zero head wind velocity.

In the series hybrid system, the electric motor behaves exactly in the same manner as in an electric vehicle. In both cases, the electric motor provides the necessary power to the drive shaft. Whereas, in the case of the parallel hybrid vehicle, the necessary wheel power is provided by the ICE and the electric motor. Therefore, the torque and power requirements of the electric motor are roughly equal for EV and series hybrid, while due to power sharing they are comparatively lower for parallel hybrid. The amount of power sharing in parallel hybrid, however, depends on the relative size of the ICE and the electric motor, and on the control strategy. In this study, the system mode of control assumes the ICE is providing the base power for cruising the vehicle, and the electric motor is used to provide the peak power during acceleration and hill climbing [13]. The ICE size is determined based on this mode of control. The electric motor size, however, depends on the particular motor in use, on the optimal motor control, and also on the above mentioned system mode of control. The detailed analysis of it can be found in [7].

In the calculation of the conduction and switching losses of the converter, PWM operation with hard switching is considered. The maximum switching frequency is assumed to be 10 kHz. The voltage and current rating of each switch of the inverter module used in the simulation are 600V and 400A respectively. For the calculation of the switching loss, the manufacturer's data on the switch turn on and turn off profiles, including reverse recovery effects of anti-parallel diodes, are used. The on-state characteristic of each switch module is simulated by a dc source, representing the saturation voltage, in series with an on-state resistance. This simplified model is used for the calculation of the conduction loss. The control strategy, the pf of operation, and the high speed-constant power capability are different for each type of motor. Consequently, the converter losses will be different for each case. In the simulations, IM, BLDC motor, and SRM are considered. Torque control below the base speed is achieved through the PWM chopping of current. As mentioned earlier, to maximize the available torque at high speed, phase control of the input voltage is used to control the torque. This control technique has the advantage of requiring only few switchings per electrical cycle. On the other hand, it has the disadvantages of being sluggish in response and having higher torque ripple. These drawbacks, however, are expected to have minimal effect on the vehicle operation due to the high vehicle inertia. Simulation results of the converter losses are presented in the next section.

IV. Simulation Results

In this section, the converter switching and conduction losses of a simulated electric and hybrid electric vehicle are calculated. For both systems, the cases when the vehicle runs on the FTP75 urban drive cycle (Fig. 1(a)) and on the highway drive cycle (Fig. 1(b)) are studied.

A. Losses in an HEV

The converter losses in an HEV depend on the energy sharing between the ICE and the electric motor. Figures 2(a) and 2(b) show the total energy through put and the energy distribution between the ICE and the electric motor, when the vehicle is running in the two drive cycles. In these figures, the energies are calculated cumulatively by integrating each power component over the drive cycle time. It is possible to recover, at least partially, the kinetic energy released by the vehicle when it decelerates. This is achieved by running the electric motor as a generator and charging the battery pack. This mode of control is referred to as regenerative braking in the literature. For obvious reason, the regenerative braking energy, which has its associated converter losses, is considered positive. This energy is added to the electric motor energy. In this analysis, it is assumed that all the kinetic energy released during the vehicle deceleration is recovered through regeneration, except for the amount lost in the process of regeneration. However, this is not practical for a very rapid braking of the vehicle. The electric motor and the battery pack are not capable of handling the huge amount of power released in a short burst during the harsh braking. In that case the mechanical brake needs to be engaged in addition to the regenerative braking. However, for the drive cycles considered in this study (Figs. 1(a) and 1(b)), the above assumption is valid. It is obvious, from the simulation results of Fig. 2(a), that the energy flow through the electric motor of the hybrid vehicle, running in highway drive cycle, is extremely small when compared to the total energy. Any amount of energy savings, by soft switching, in this case will not have much impact on the total energy savings. The urban drive cycle (Fig. 1(b)), however,

requires the electric motor more frequently, to supply the acceleration power of the hybrid vehicle. Moreover, the energy released during vehicle deceleration in the urban drive cycle is also recovered by the electric motor (generator), converter set.

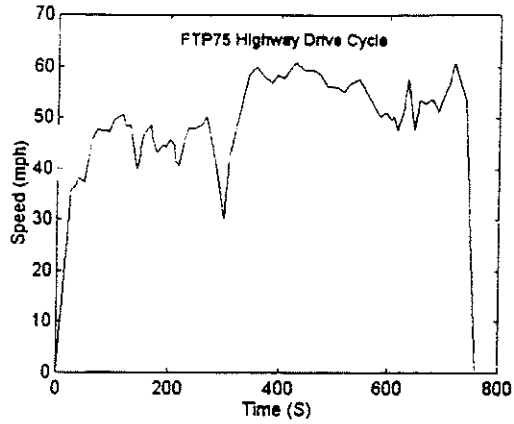

(a)

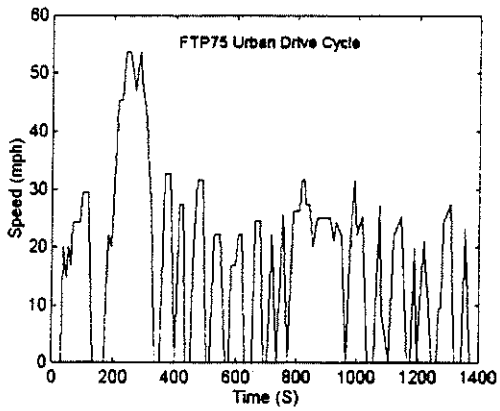

(b)

Fig. 1. FTP75 highway (a) and urban (b) drive cycles.

In the case of EV, since the battery is the only source of energy, the total energy required to run the vehicle is handled by the electric motor. Special assessment of energy savings due to soft switching is, therefore, necessary for the EV operation in both drive cycles. For the HEV operation, it might be important only in the urban drive cycle.

The calculated values of the conduction (the solid line curve) and switching (the dashed curve) losses of HEV drivetrain systems using IM, BLDC, and SRM are presented in Figs. 3(a) and 3(b) for the urban drive cycle. Fig. 3(a) considers the case when the vehicle deceleration energy is recovered through regenerative braking, and Fig. 3(b) is for the case when the regeneration is not considered. The losses of Figs 3(a) and 3(b) are shown as a percentage of the total expended energy of the propulsion system. The converter energy losses and the total energy are calculated cumulatively, integrating the losses and the system power over the drive cycle time. Hence, loss percentage shown at any point in these figures indicates the average loss (in percent) up to that time of the drive cycle. The losses shown at the end of the drive cycle are, therefore, the average losses for the whole drive cycle. In figures 3(a) and 3(b) we can see two spikes at the beginning of the drive cycle. These spikes are due to the two initial accelerations of the vehicle. As time progresses, the cumulative energy builds up and any local fluctuation, due to subsequent car accelerations, does not show up in the global

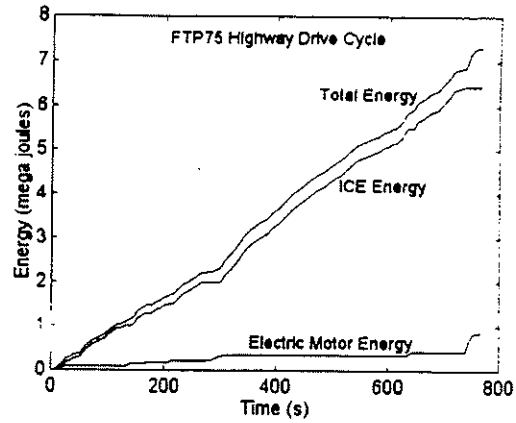

(a)

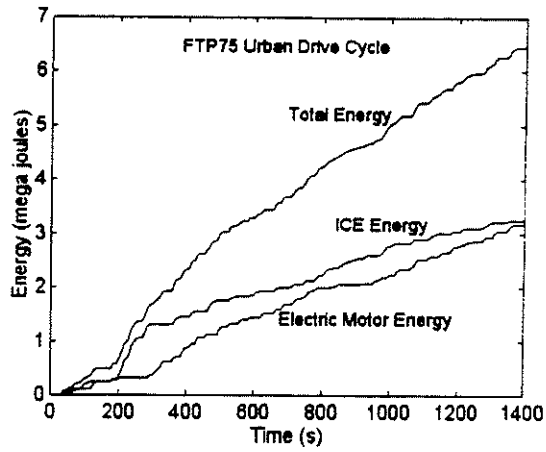

(b)

Fig. 2. Energy consumption in HEV for highway (a) and urban (b) drive cycles.

picture. Due to the lower pf of operation of SRM, its conduction loss is higher in both cases. However, the switching loss of SRM converter is comparable to those of IM and BLDC inverters. High speed capability of SRM, besides the fact that the torque control at high speed is attained by the phase control of the input voltage, have helped to lower the switching losses in SRM converter, despite its lower pf of operation. For the HEV urban drive cycle the average switching losses (Fig. 3(a) and Fig. 3(b)), for all motors considered here, are less than 2% of the total energy for the case with regenerative braking and less than 1% for the case without regenerative braking. In some soft switched topologies the conduction loss can be higher than in a hard-switched converter [14]. Although the switching loss can be reduced considerably, it is not totally eliminated. Hence, if one assumes zero switching losses by using a soft switching

technique, for this drive cycle, the maximum gain in energy would, therefore, be less than 2%.

Now, let us examine the impact of soft switching on the operation of HEV in terms of the gasoline saved per 100 miles of travel. The total energy spent for the operation of the vehicle in

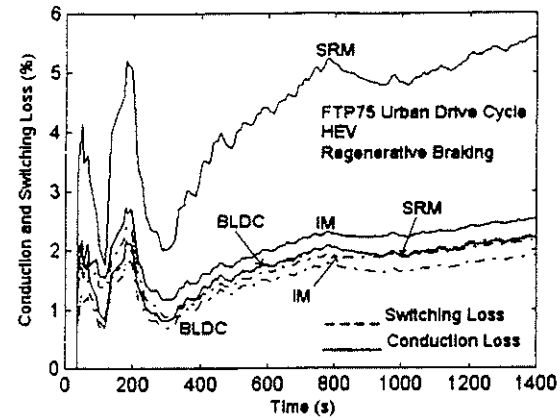

(a)

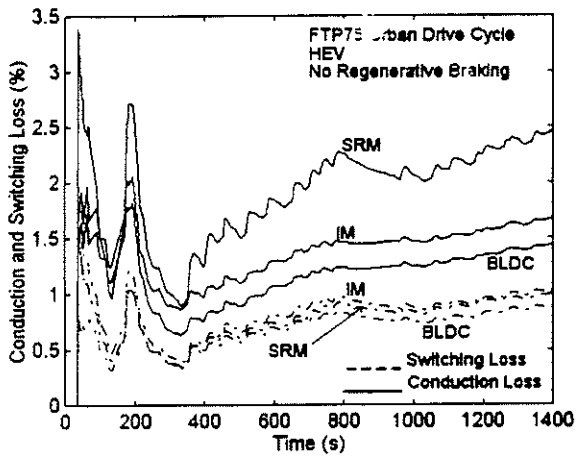

(b)

Fig.3. Converter losses for HEV in urban drive cycle with (a) and without (b) regenerative brakings.

the urban drive cycle is 6.45 mega joules. Total distance traveled by the vehicle in this drive cycle is 6.6 miles. Energy density per gallon of gasoline is 121 mega joules. Assuming an efficiency of 20% in the operation of the ICE, the total savings in the gasoline is only 0.0808 gallons per hundred miles traveled in the urban drive cycle. Total savings for an average urban driving of 10,000 miles in a year is only 8.08 gallons of gasoline. Since HEV is not energy limited, we conclude, the extra cost and complexity associated with the operation of a soft switched converter do not justify soft switching for HEV.

In highway driving cycle, except for few accelerations and few cases of regenerative braking, the electric motor is seldomly used . Calculated values of the switching losses for the operation of HEV in the highway drive cycle are shown in Figs. 4(a) and 4(b) with and without the consideration of regenerative braking, respectively. These losses are not significant and do not warrant any special effort in converter efficiency improvement.

B. Losses in EV

The energy recovered through regenerative braking is the same in EV as in HEV. However, since the battery is the only source of energy, the energy flow out of the battery pack is higher in case of EV. Due to this increased energy flow through the electric motor, the converter incurs more losses in both conduction and switching. Hence, losses as a percent of total energy is higher in case of EV. This is shown in Fig. 5(a) and 5(b) for urban driving cycle with and without the consideration

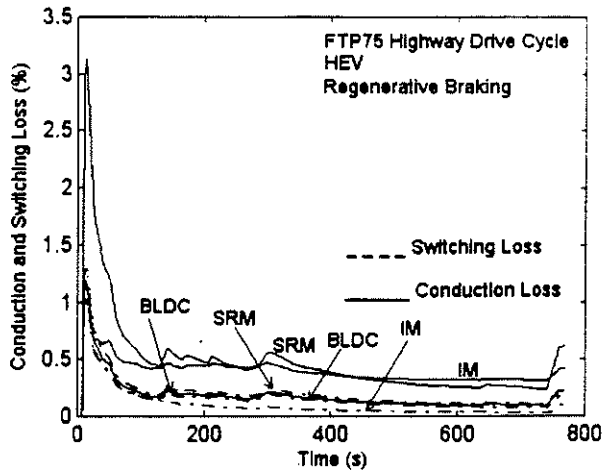

(a)

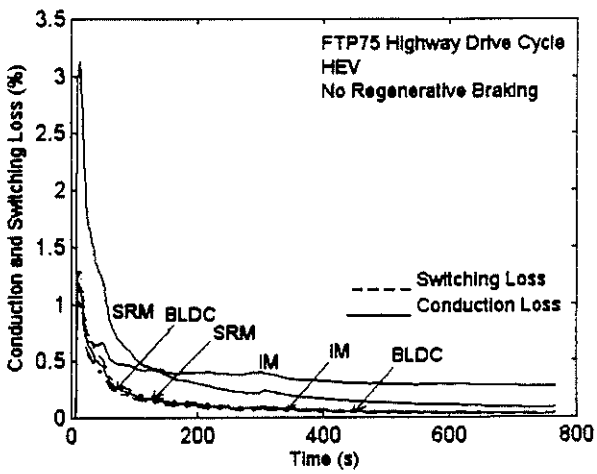

(b)

Fig.4. Converter losses for HEV in highway drive cycle with (a) and without (b) regenerative brakings.

of regenerative braking respectively. In both cases the switching and the conduction losses are increased for the operation of EVs when compared to those of HEVs. The switching loss is close to 3% with regenerative braking and close to 2% without regenerative braking. Although, the losses in EV are not greatly increased compared to the losses of HEV, EV losses have severe

consequences since they are related directly to the range of the vehicle. Therefore, the energy savings through soft switching may justify the additional cost, complexity, and lower reliability associated with its operation.

Finally, we consider the highway driving for EV. Although, EVs are not best suited for highway driving, the losses can be calculated for completeness. Figs. 6(a) and 6(b)

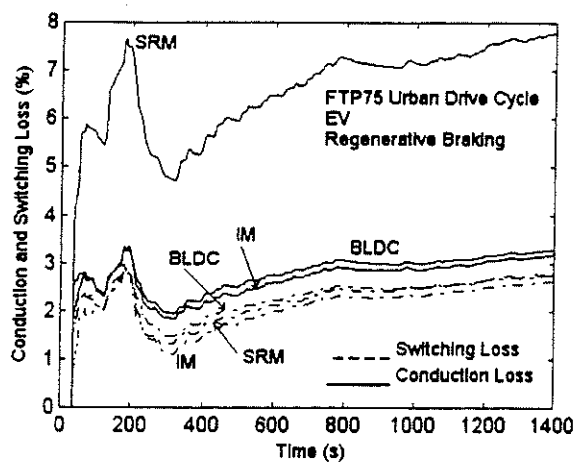

(a)

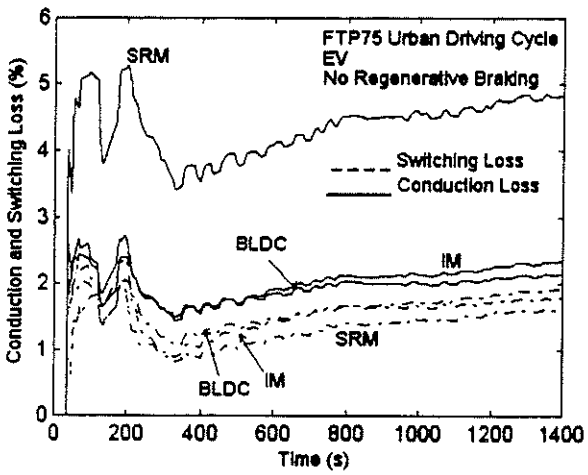

(b)

Fig.5. Converter losses for EV in urban drive cycle with (a) and without (b) regenerative brakings.

show the converter losses for the operation of the EV in the highway drive cycle with and without the consideration of the regenerative braking. Since the electric motor (battery) supplies all the energy in the operation of the EV, the losses are higher than in the case of HEV operation in the same drive cycle. However, the switching loss percentage is lower in highway driving as compared to the city driving of the EV (Figs. 5(a) and 5(b)) . It can be seen in Figs. 6(a) and 6(b), that the switching losses are actually less than 1% in both cases. The energy savings in the hypothetical highway driving of EV, therefore, may not justify the adoption of soft switching for its driving in the highway cycle.

V. Discussion

The simulation results of section IV give little incentive for soft switching in HEV, as far as the efficiency of the drivetrain is concerned. However, EV is a different issue. Since

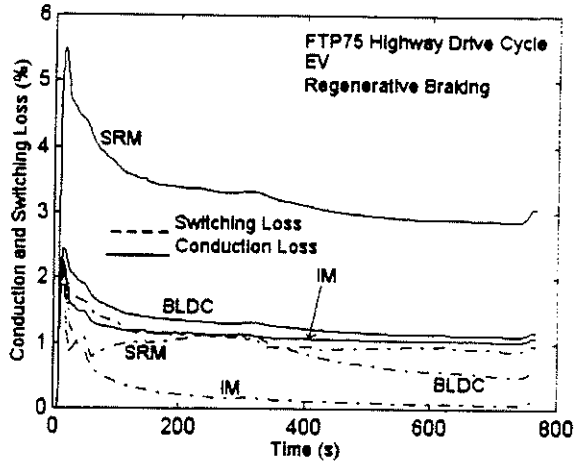

(a)

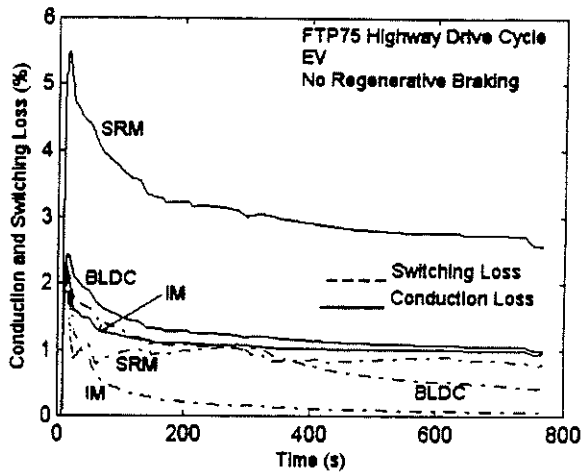

(b)

Fig.6. Converter losses for EV in highway drive cycle with (a) and without (b) regenerative brakings.

EV is energy limited, any gain in efficiency, by adopting soft switching, is directly related to the range of the vehicle. Hence, the marginal 3% gain in efficiency shown in the previous section for the urban driving cycle still may justify soft switching for EV electrical drive train. In other papers, e.g., [6] , the soft switching operation is shown to provide more gain in the efficiency of the converter than it is shown here. Those results should not be confused with the concepts presented in this study. Here we have evaluated the converter efficiency from the system prospectives. The gain in efficiency shown in this paper is based on the specific application to EV and HEV drivetrains with a special (optimal) mode of control, especially at the high speed operation of the vehicle (motor), as opposed to the fixed

frequency PWM switching operation for a fan or resistive load used in the other works.

Faster switches are developed to reduce the switching power losses. However, the high di/dt and dv/dt associated with the faster switching cause voltage and current spikes due to stray inductance and capacitance in the circuit. This phenomenon causes high current and voltage stresses in the switch, and can also produce severe EMI problems. The use of snubbers can reduce the switching stresses in the switches, but they are lossy and add parts count. Another approach, as suggested in [8], is to use slower switches for vehicle applications. This would reduce both the EMI problem and switch stresses. But it will increase the switching losses. The additional switching losses caused by the slower switches should not have much impact on the operation of the HEV, however, it may favor soft switching for EV applications.

Soft switching with high switching frequency can produce a fast converter dynamic response. This may be difficult to achieve with hard switching without sacrificing efficiency. However, vehicle has a slow dynamics. Faster dynamic response, therefore, is not necessary from the electrical propulsion system of the EV and HEV. On the contrary, a deliberate damping may be required to suppress the possible excitation of any mechanical resonances [15].

Slower switching, in an attempt to reduce the switching losses, will introduce higher torque and current ripples. Nevertheless, the vehicle inertia is expected to smoothen the effect of torque ripple on the speed ripple.

The audible noise for switching at frequencies lower than 20 kHz is another issue. Switching over 20 kHz with hard switching may not be practical for high power drives. The audible noise, however, may not be unacceptable to the users who are already accustomed to the noisy operation of the conventional automobiles. It may also be particularly tuned to be pleasant to the ear.

VI. Conclusions

An evaluation of the soft switching inverters for EV and HEV motor drives is presented. Simulation results of the converter losses are presented for the operation of the EV and the HEV in the FTP75 city and highway drive cycles. Operation of induction, brushless dc, and switched reluctance motors are considered for the electrical propulsion system of the EV and the HEV. The simulation results show that the energy savings by using soft switching is less than 2% of the total energy for the operation of the HEV in the standard highway as well as in the urban driving cycles. Since, HEV does not have any energy limitation, this small saving in energy does not justify the extra cost and complexity associated with the soft switched converter. The simulation results for the operation of the EV in the urban driving cycle reveal that the maximum savings in energy would be up to 3% with soft switching. These savings, although marginal, may justify soft switching for EV applications until high energy density batteries with extremely quick charging characteristics are developed in the future. The energy savings for EV with soft switching in highway driving is less than 1% of the total energy. Since, EVs are not designed for primary highway driving, the small energy savings may not justify soft switching for this case. We can summarize our findings as follows:

- Soft switching is not recommended for the design of HEV.
- Soft switching is not recommended for the design of EV in highway driving.
- Soft switching may be recommended for EV operation in urban driving. However, a specialized soft switched topology would be needed for the particular vehicle load.

To reduce the EMI problem and the switch stresses due to fast switch turn-ons and turn-offs, slower switches may be used. The additional losses incurred by these slow switches are not expected to have any major impact on the operation of the electrical propulsion system of the HEV. The other characteristics of soft switching with high switching frequency such as, faster dynamic response, torque and current ripple, audible noise etc., do not have any appreciable effect on the design and operation of the EVs and the HEVs.

VII. REFERENCES

[1] Y. Murai and T. A. Lipo, "High Frequency Series Resonant DC Link Power Conversion", *IEEE IAS Annual Meeting Conference Record*, 1988, pp. 772-779.

[2] D. M. Divan, "The Resonant DC Link Converter - A New Concept in Static Power Conversion", *IEEE Transactions on Industrial Applications*, Vol.25, No.2, pp. 317-325, 1989.

[3] William McMurray, "Resonant Snubbers with Auxiliary Switches", *IEEE Transactions on Industry Applications*, Vol.29, No.2, March/April 1993.

[4] M. Ehsani and T. S. Wu, "Zero Current Soft Switched Capacitively Coupled DC-AC Converter for High Power", *IEEE Industry Application Society Annual Meeting Records*, Toronto, pp. 800-805, 1993.

[5] T. S. Wu, M. D. Bellar, A. Tchamdjou, J. Mahdavi and M. Ehsani, "A Review of Soft-Switched DC-AC Converters", *IEEE IAS Annual Meeting Conference Record*, 1996, Vol.2, pp.1133-1144.

[6] J. S. Lai, "Resonant Snubber-Based Soft-Switching Inverters for Electric Propulsion Drives", *IEEE Transactions on Industrial Electronics*, Vol. 44, No.1, pp. 71-80, February 1997.

[7] M. Ehsani, K. M. Rahman, and H. Toliyat, "Propulsion System Design of Electric and Hybrid Vehicle," *IEEE Trans. on Industrial Electronics*, vol. 44, no. 1, pp.19-27, February 1997.

[8] X. Xu, V. A. Sankaran, "Power Electronics in Electric Vehicles: Challenges and Opportunities," *IEEE IAS Annual Meeting Conference Record*, 1993, pp. 463-469.

[9] T. J. E. Miller, "Switched Reluctance Drive," Short Course, *IEEE-IAS* Conference, Seattle, 1990.

[10] T. M. Jahns, "Torque Production in Permanent Magnet Synchronous Motor Drives with Rectangular Current Excitation," *IEEE Trans. Industry Application*, vol. 20, no. 4, pp. 803-813. July/Aug., 1984.

[11] R. C. Becerra and M. Ehsani, "High Speed Torque Control of Permanent Brushless DC Motors," *IEEE Trans. Industrial Electronics,"* vol. IE-35, no. 3, pp. 402-406, August, 1988.

[12] C. C. Chan, J. Z. Jiang, G. H. Chen, X. Y. Wang, and K. T. Chau, "A Novel High Power Density Permanent Magnet Motor Drive for Electric Vehicles," in *Proc. EVS11*, paper 8.06, 1992, pp.1-12.

[13] Y. Gao, K. M. Rahman, and M. Ehsani, "Parametric Design Of The Drive Train Of Electrically Peaking Hybrid (ELPH) Vehicle," *SAE Journal Publication SP-1243, paper no. 970294*, 1997.

[14] J. S. Lai, R. W. Young, and J. W. McKeever, "Efficiency Consideration of DC Link Soft-Switching Inverters for Motor Drive Applications," *IEEE PESC Annual Meeting*, 1994

[15] H. A. Toliyat, K. M. Rahman, and M. Ehsani, "Electric Machines in Electric and Hybrid Vehicle Applications," *ICPE*, Seoul, Korea, 1995.

Fundamentals of Energy and Power Storage and Production in HEV Architectures

Stephen W. Moore
Texas A&M University

Mehrdad Ehsani
Texas A&M University

ABSTRACT

Fundamentals of hybrid electric vehicle architecture and component selection are presented in this paper. Current hybrid and electric vehicle topologies include numerous architectural arrangements ranging from the all-electric drive to parallel and series types. Each architecture features a novel arrangement of engines, motors, batteries, or some other source of varying different sizes. However, each architecture can be abstracted into basic concepts of power production and energy storage.

This paper presents a fundamental concept of designing a vehicular hybrid drivetrain by separating the concepts of power and energy production and storage. A fundamental drive cycle featuring the basic building blocks of vehicle performance is presented and analyzed. The boundaries for maximum and minimum transient power expenditures and absorption are established. Total energy consumption, generation, and storage requirements are identified.

Each individual drivetrain component's power and energy production and storage characteristics are identified and are combined in such a way to satisfy the vehicle's performance criteria. A series hybrid is presented as an example of the conceptual separation of power and energy for a given drive cycle.

INTRODUCTION

The hybrid automotive drivetrain can be conceptually abstracted into two components: a power source and an energy source. The power source is responsible for instantaneous transients such as providing brief power for accelerations or regenerative braking and for passing maneuvers or hill climbing. The energy source is responsible for contributing average power. These concepts are most easily illustrated with a series hybrid (Figure 1) [1].

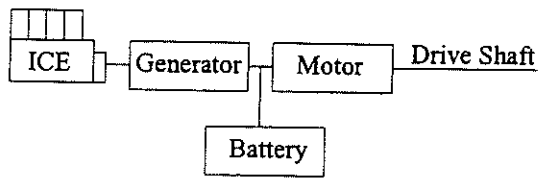

Figure 1. Series Hybrid Architecture

The series hybrid is much like an electric vehicle with the exception of on-board electricity production. The ICE and generator produce the average energy requirement of the vehicle and additional transient power is provided by the battery pack. This architecture will be studied more in the next section. Notice that the series hybrid is not limited to ICE and generator. Many options exists such as fuel cells, thermoelectric cells [2], and turbine generators.

The traditional method used to evaluate or simulate vehicle performance is with the use of a drive cycle. A drive cycle is a set of pre-defined driving profiles with different performance requirements that can be used to represent the majority of driving expectations. There are many popular drive cycles available varying in intensity and length (Table 1)[3]:

Table 1. Various US Drive Cycles

Name	Abbreviation	Time (sec)	Length (km)
EPA Highway Cycle	HWY	765	16.5
EPA City Cycle	LA4	1372	12.0
Unified LA92 Cycle	LA92	1435	15.8
New York City Cycle	NYCC	599	1.9
US06 Cycle	US06	600	12.9

Please notice that the EPA City Cycle LA4 is also known as the FTP cycle, or the Federal Urban Driving Schedule (FUDS). The LA4 was developed in the early 1970s to simulate urban driving conditions. Later urban driving scenarios include the California Air Resources Board Unified LA92 Cycle [4], developed in 1992. The

US06 was developed by the EPA to include some additional features over the earlier LA4 [5]. Pictured below is the LA4 driving cycle.

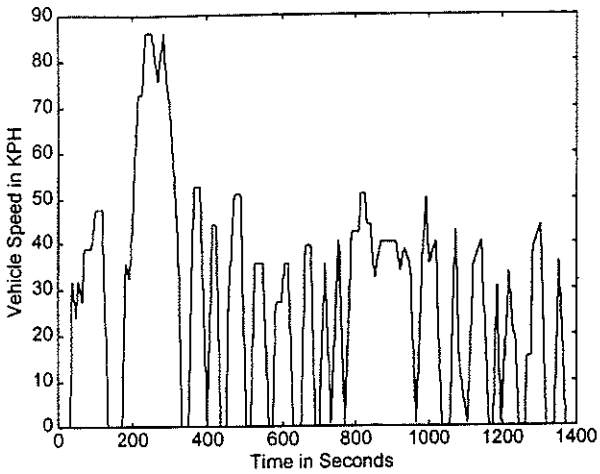

Figure 2. EPA City Cycle LA4

Other countries and agencies have developed similar driving cycles for testing and evaluation purposes. However, it is presented that all driving cycles share three common characteristics:

1. Maximum and minimum power transients.
2. Average energy consumption.
3. Maximum deviation between instantaneous power consumption and average energy production.

These three characteristics will be evaluated in the following sections.

VEHICLE DYNAMICS MODEL

To illustrate the concept of abstracting a drive cycle into power and energy characteristics, a simplified vehicle model is used. The vehicle load (F_w) consists of rolling resistance (f_{ro}), aerodynamic drag (f_l), and climbing resistance (f_{st}) [6].

$$F_w = f_{ro} + f_l + f_{st} \qquad \text{(Eq. 1)}$$

The rolling resistance (f_{ro}) is caused by the tire deformation on the road:

$$f_{ro} = f \cdot m \cdot g \qquad \text{(Eq. 2)}$$

where f is the tire rolling resistance coefficient. It is nonlinear and increases with vehicle velocity, and also during vehicle turning maneuvers. These nonlinearities are not taken into account in this model. Vehicle mass is represented by m, and g is the gravitational acceleration constant.

Aerodynamic drag, f_l, is the viscous resistance of air acting upon the vehicle:

$$f_l = 0.5\xi C_w A(v + v_0)^2 \qquad \text{(Eq. 3)}$$

where ξ is the air density, C_w is the aerodynamic drag coefficient, A is the vehicle frontal area, v is the vehicle speed, and v_0 is the head wind velocity.

The climbing resistance (f_{st} with positive operational sign) and the down grade force (f_{st} with negative operational sign) is given by

$$f_{st} = m \cdot g \cdot \sin\alpha \qquad \text{(Eq. 4)}$$

where α is the grade angle.

A typical simplified road load characteristic as a function of vehicle speed is shown in Figure 3.

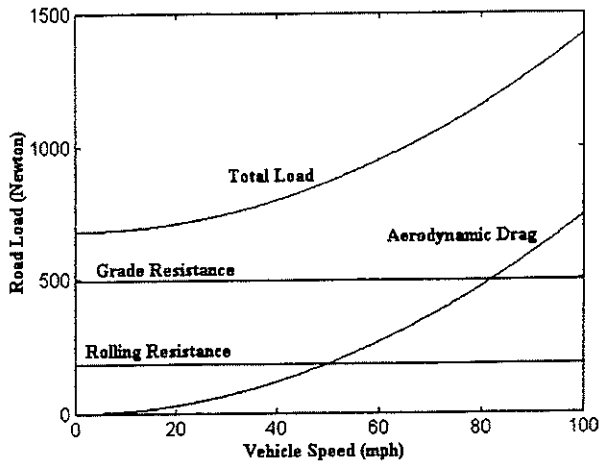

Figure 3. Typical Vehicle Load Function

This graph represents the load function of the vehicle with the characteristics of Table 2. Notice that this graph does not take into account a headwind, a variable grade, or the nonlinearities of tire deformation and rolling resistance.

Table 2. Example Vehicle

Parameter	Value
Mass	1450 kg
Rolling Resistance Coefficient	0.013
Aerodynamic Coefficient	0.29

SERIES HYBRID EXAMPLE

A simple series hybrid topology was simulated using the LA4 drive cycle to examine power and energy consumption. Figure 4 illustrates the kinetic energy of the vehicle during the drive cycle:

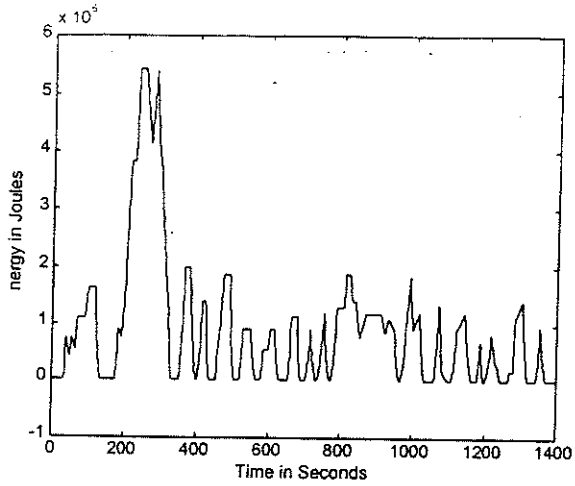

Figure 4. Kinetic Energy of the Vehicle

Adding in the aerodynamic and rolling resistance losses, the total amount of energy the vehicle consumes over the drive cycle can be plotted (Figure 5):

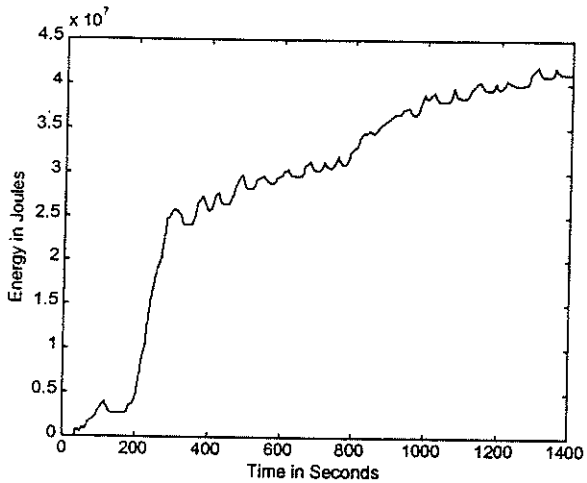

Figure 5. Cumulative Vehicle Energy Consumption

Taking the derivative of the energy consumption we can size the traction motor for the peak power requirement (Figure 6):

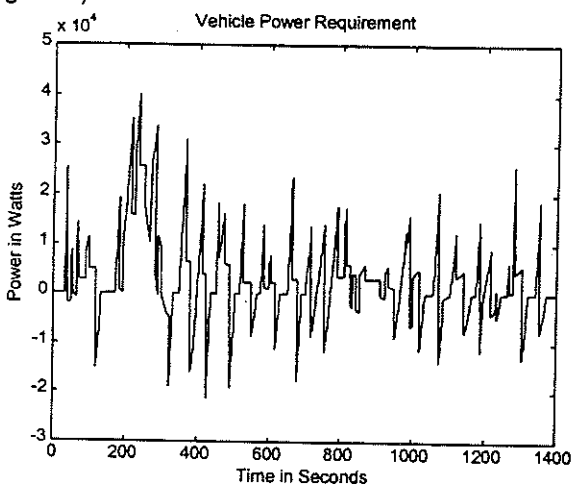

Figure 6. Instantaneous Power Requirement

Thus this vehicle requires a 41 kW peak power traction motor capable of 22 kW of regeneration to perform adequately on the LA4 driving cycle in zero wind, zero grade conditions. Looking at Figure 5, we see that the average energy consumption was 1.7e+7 joules, which means an average power consumption of 29 kW. Thus the traction motor must be sized to continuously dissipate the heat associated with the average load in addition to the heat produced by the peak loads.

Assuming that this series hybrid has an ICE and generator producing electrical energy at a continuous rate equal to the average consumption (29 kW), a plot of the cumulative energy production and the cumulative energy consumption can be made (Figure 7):

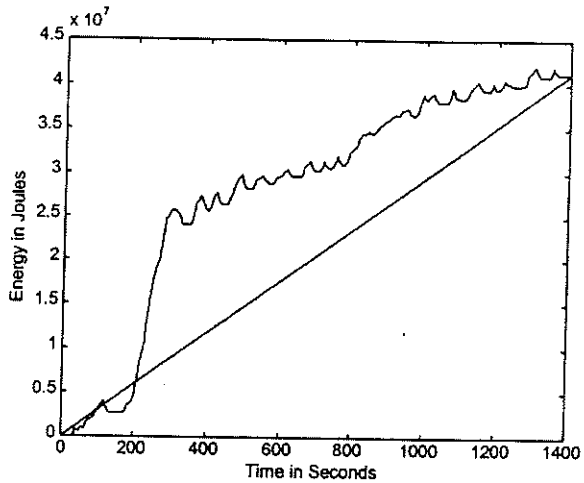

Figure 7. Energy Consumption and ICE Production

Notice how the ICE/generator energy production *exactly equals* the energy consumption of the vehicle. However, because the ICE/generator produces energy at a constant rate and the vehicle consumes energy at a variable rate, a transient energy storage device (the 'battery,' or some other type of storage device) is required. Illustrated on Figure 8 is the amount of energy stored in the battery of the vehicle (assuming the battery is at zero condition at the beginning of the cycle):

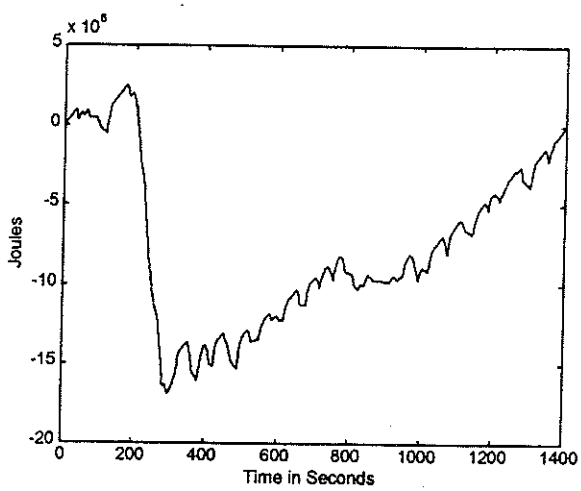

Figure 8. Energy Content of Battery

The battery discharges rapidly with the initial acceleration and cruise in the LA4 profile, then is slowly recharged by the series ICE/generator. The power requirement of the battery can be found by taking the derivative of the battery energy balance (Figure 9):

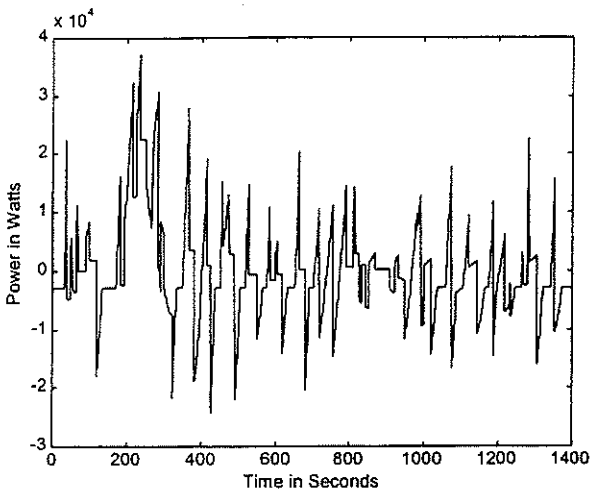

Figure 9. Power Requirement of Battery

Thus with an ideal (100% efficient) energy storage device, this vehicle will require a battery with 1.7e+7 Joules (4695 watt-hours) of storage and be able to stand 39 kW watt discharge and 25 kW (depending on regenerative braking performance as well) recharge power. The ICE/generator produces 29 kW continuously. Using a non-ideal energy storage device (a simplified ultracapacitor model was used for this scenario), the energy loss is apparent (Figure 10):

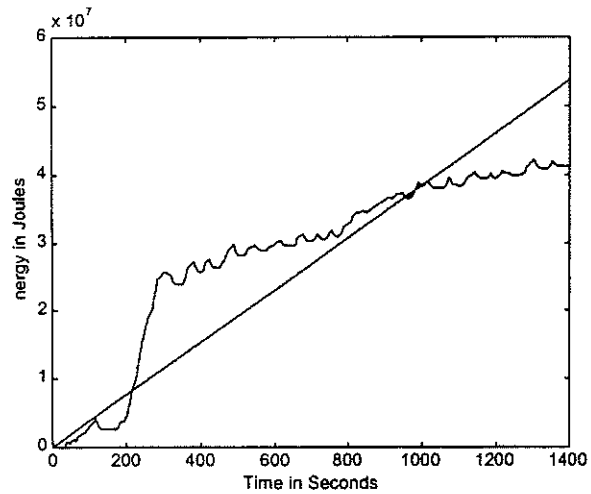

Figure 10. Vehicle Energy Consumption and ICE Production

Notice that the ICE/generator is required to produce more energy than the vehicle dynamics consume to compensate for losses in the energy storage device. The peak power and energy capacity criteria of the storage device are also increased (up to 44 kW peak discharge power and 5.2 kWhr capacity).

DRIVE CYCLE ANAYLSIS

As discussed in the introduction, drive cycles share three common characteristics:

1. Maximum and minimum power transients.
2. Average energy consumption.
3. Maximum deviation between instantaneous power consumption and average energy production.

Inspection of Figure 6 reveals that the series hybrid with the characteristics of Table 2 has a maximum peak power of 41 kW. Figure 5 illustrates the cumulative energy consumption, which can be divided by the total time to find the average energy consumption of 29 kW. Figure 7 illustrates the difference between the cumulative energy consumption and the cumulative energy production. The maximum difference between these two values at any time denotes how much energy the vehicle must store above average to deliver power for peak loads. In this example, the maximum deviation is 1.7e+7 joules for the ideal case and 1.9e+7 joules for the non-ideal case.

Each of these values relate to component sizing. The traction drive motor must be capable of 41 kW peak power and 29 kW of average power. The ICE/generator must be capable of producing 29 kW continuously and the battery must be at least 4.7 kWhr in size (ideal case example). Many series hybrid implementations allow for the ICE to operate intermittently. In this case, the ICE must produce an average of 29 kW over its on/off cycle, and the battery capacity must be increased to accommodate operating the vehicle then the ICE is not operating. Under these conditions, the battery peak charge and discharge rates will also be much higher, because the battery will be supplying all the power to the traction motor during the ICE off cycle.

This type of analysis can be implemented on any hybrid architecture, series or parallel. In parallel operation, the energy production always comes from the ICE, but the ICE also serves as a traction (power) device as well.

Several drive cycles that appear to be vastly different may exhibit similar characteristics when analyzed in this fashion. Drive cycle top speed is a serious issue in aerodynamic and maximum component RPM ratings, but becomes irrelevant in this type of analysis. Two different drive cycles with different top speeds may compute to be equal in terms of maximum power and energy consumption. In this case, the traction motor peak power, ICE/generator sizing and battery capacity requirements are all the same. However, in the case of the drive cycle with the higher top speed, the traction motor must be rated to the proper RPM.

CONCLUSIONS

Any hybrid vehicle architecture can be broken down into two abstract components: energy and power storage and production. Each drivetrain component contributes one or both of these elements. A simplified series hybrid example was presented in which the energy consumption of the vehicle was compared to the energy production of the ICE/generator. The difference in these energies was identified as the amount of energy the vehicle's battery would have to store. In addition, the amount of energy the ICE/generator would have to produce was identified, as well as the maximum peak power requirement of each component

The EPA LA4 drive cycle (the Federal Urban Driving Schedule) was used as an example drive cycle in this illustration. However, the specifics of the LA4 cycle are irrelevant in this type of analysis, because a drive cycle with vastly different characteristics could very well show the same results, as long as it required the vehicle to consume the same amount of average energy and have a similar global maximum power requirement. However, some specific features of the drive cycle are important for other considerations, such as aerodynamics or component RPM ratings.

This method of analyzing system energy and power flow can be applied to other HEV architectures other than series. Hybrid architectures which incorporate an energy storage device such as a battery or ultracapacitor fall in this category.

REFERENCES

1. A.F. Burke, "Hybrid/Electric Vehicle Design Options and Evaluations," SAE Paper 920447.
2. Michael Seal, et al., "Thermophotovoltaic Generation of Power for Use in a Series Hybrid Vehicle," SAE Paper 972648.
3. Feng An, M. Barth, and G. Scora, "Impacts of Diverse Driving Cycles on Electric and Hybrid Electric Vehicle Performance," SAE Paper 972646.
4. T. Austin, et al., "An Analysis of Driving Patterns in Los Angeles During 1992," Proceedings of the Third Annual CRC-APRAC On-Road Vehicle Emissions Workshop, San Diego, CA, 1992.
5. US Document, "Support Document to the Proposed Regulations for Revisions to the Federal Test Procedure: Detailed Discussion and Analysis," EPA Office of Air and Radiation, 1995.
6. Automotive Handbook, Germany: Robert Bosch Gmbh, 1986.

Effect on Vehicle Performance of Extending the Constant Power Region of Electric Drive Motors

Stephen W. Moore
Texas A&M University

Khwaja M. Rahman
Texas A&M University

Mehrdad Ehsani
Texas A&M University

ABSTRACT

The effect on vehicle performance of extending the constant power operating mode of electric drive motors for electric and hybrid vehicles is presented in this paper. Modern electric and hybrid vehicle designers have the selection of several technologies to choose from when selecting an electric drive motor. Each motor technology exhibits a particular torque vs. speed characteristic. Many of these technologies, most notably the switched reluctance machine, have capitalized on iron and copper utilization, extending their useful speed range. However, the extended speed capabilities of these motor drives have vehicle performance consequences.

It is presented that vehicle performance is affected by changing the torque-speed characteristics of the drive motor. The extended constant power speed range motor can have smaller rated power than otherwise but suffer high speed passing performance. Traditional extended constant power range motors (about two times the rated speed) have to have a higher rated power but exhibit superior performance capability.

INTRODUCTION

The electric motor is of primary importance to the electric and hybrid vehicle designer. In an electric or a series hybrid vehicle the electric drive is the only propulsion mechanism and much attention needs to be paid to cost, weight, and performance. Depending on the architecture, electric motor drives in parallel hybrid designs can be utilized as peak power devices, load sharing devices, or only as a small transient torque source. Some parallel hybrid concepts even allow the drivetrain to revert to an electric-only mode, relegating all propulsion to the electric drive. In parallel applications like these, the motor technology is equally critical as in the cases of EV or series HEVs.

An electric motor can operate in two modes, the normal mode and the extended mode (Figure 1). In the normal mode, or the constant torque region, the motor exerts constant torque (rated torque) over the entire speed range until the rated speed is reached. Once past the rated speed of the motor, the torque will decrease proportionally with speed, resulting in a constant power (rated power) output. The constant power region eventually degrades at high speeds, in which the torque decreases proportionally with the square of the speed. This is known as the 'Natural Mode' and is usually neglected for most motor technologies. Please note that Figure 1 denotes a 1:3 type motor, where the constant power region extends beyond the constant torque region by a factor of 3.

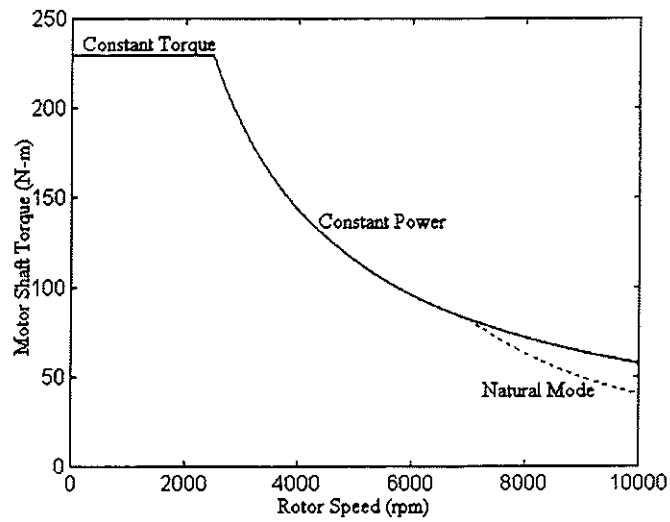

Figure 1. Typical Motor Characteristics

Three major motor technologies were chosen for illustrative purposes: the induction motor, the brushless DC (BLDC) motor, and the switched-reluctance (SRM) motor. Specifications for each motor technology were chosen from commercially available samples, and do not represent maximum possible performance for each technology.

	Rated Speed	Maximum Speed	Power Ratio
Induction	1750	8750	1:5
BLDC	4000	9000	1:2.25
SRM	4000	20000	1:3

Table I. Electric Motor Technologies

It must be noted that the SRM is capable of operating in the natural mode up to 20,000 rpm.

Induction machine drives are the present leading technology for EV and HEV power trains [1,2]. Both the GM EV-1 and Nissan FEV employ the induction motor. Permanent magnet (PM) motors are particularly known for their high efficiency and high power density. PM motors can be broadly classified into sinusoidally fed PM synchronous motor (PMSM) and rectangular fed brushless dc (BLDC) motor. The high efficiency of operation of these motors has attracted EV applications. Specially designed varients of these motors are used in the BMW E1/E2 and U2001, whereas the Ford/GE ETX-II use PMSM motor [3-5]. The major shortcoming of PM motors is the cost due to the high energy magnets. Safety is another issue because the PM field may cause severe consequences during a short circuit fault [6]. BLDC motors suffers from poor field weakening capability due to the surface mounting of the permanent magnet field that may necessitate a multi-gear transmission with the operation of this motor [6]. The interior magnet PMSM motor has reluctance torque in addition to reaction torque and this may help in getting a long constant power operation [7]. However, interior mounting of the permanent magnets further increases the cost and may reduce the maximum speed.

The switched reluctance motor is gaining lot of attention for its simplicity and safe operation. This motor is commercially used in the Chloride Lucas EV. Test results showed superior operation and higher power density when compared to an induction motor [8]. Because of its simple construction and low rotor inertia, the SRM has very rapid acceleration and extremely high speed operation. Because of its wide speed range operation, the SRM is particularly suitable for gearless operation in EV/HEV propulsion.

VEHICLE DYNAMICS

A simple vehicle dymanics model to evaluate vehicle performance is presented. A simplified vehicle model load (F_w) consists of rolling resistance (f_{ro}), aerodynamic drag (f_l), and climbing resistance (f_{st}) [9].

$$F_w = f_{ro} + f_l + f_{st} \qquad \text{(Eq. 1)}$$

The rolling resistance (f_{ro}) is caused by the tire deformation on the road:

$$f_{ro} = f_r \cdot m \cdot g \qquad \text{(Eq. 2)}$$

where f_r is the tire rolling resistance coefficient. It is nonlinear and increases with vehicle velocity, and also during vehicle turning maneuvers. These nonlinearities are not taken into account in this model. Vehicle mass is represented by m, and g is the gravitational acceleration constant.

Aerodynamic drag, f_l, is the viscous resistance of air acting upon the vehicle)

$$f_l = \frac{1}{2} \cdot \rho_e \cdot C_D \cdot A_f \cdot (v + v_0)^2 \qquad \text{(Eq. 3)}$$

where ρ_e is the air density, C_D is the aerodynamic drag coefficient, A_f is the vehicle frontal area, v is the vehicle speed, and v_0 is the head wind velocity.

The climbing resistance (f_{st} with positive operational sign) and the down grade force (f_{st} with negative operational sign) is given by

$$f_{st} = m \cdot g \cdot \sin\alpha \qquad \text{(Eq. 4)}$$

where α is the grade angle.

A typical simplified road load characteristic as a function of vehicle speed is shown in Figure 2.

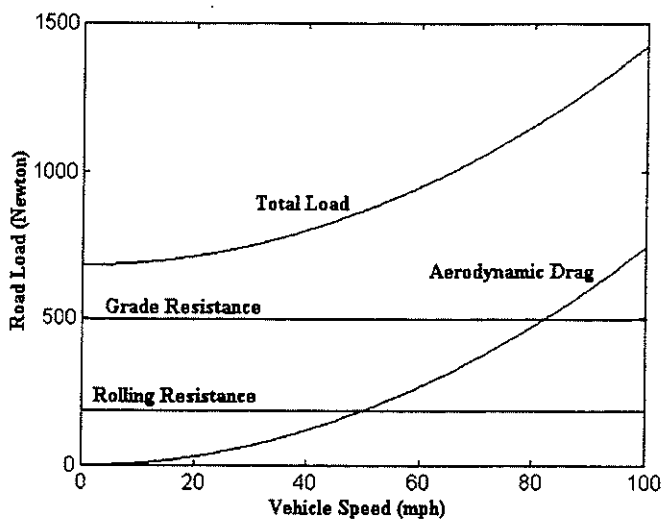

Figure 2. Typical Vehicle Load Function

This graph represents the load function of the vehicle with the characteristics of Table 2. Notice that this graph does not take into account a headwind, a variable grade, or the nonlinearities of tire deformation and rolling resistance. A gear ratio between the motor and the driveshaft is specified for a later example.

Table 2. Example Vehicle

Parameter	Value
Mass	1450 kg
Rolling Resistance Coefficient	0.013
Aerodynamic Coefficient	0.29
Gear Ratio	0.71
Wheel Radius	0.279 m

MOTOR SIZING

An electric vehicle with the basic characteristics given in Table 2 will be used to evaluate the desirability of extending the constant power range of electric machines. First, the required power must be computed. Starting with the definition of acceleration where F is defined as the amount of available propulsion force,

$$a = \frac{dv}{dt} = \frac{F}{m} \qquad \text{(Eq. 5)}$$

and integrating over a time interval t_f to a terminal velocity of v_f,

$$m\int_0^{v_{rv}} \frac{dv}{F} = \int_0^{t_f} dt \qquad \text{(Eq. 6)}$$

the rated power P_m can be found. The left hand side of the equation can be broken into separate constant torque (motor speeds up to v_{rm}) and constant power (motor speeds from v_{rm} to v_{rv}) integrals:

$$m\int_0^{v_{rm}} \frac{dV}{P_m / V} + m\int_{v_{rm}}^{v_{rv}} \frac{dV}{P_m / V} = t_f \qquad \text{(Eq. 7)}$$

Now solving for the required motor power P_m, we get:

$$P_m = \frac{m}{2t_f}(v_{rm}^2 + v_{rv}^2) \qquad \text{(Eq. 8)}$$

where the motor operates in constant torque mode until speed v_{rm} is reached, and then operates in constant power until terminal velocity v_{rv} is reached at time t_f. For our example vehicle to reach 60 mph (26.8 m/s) in 10 seconds (v_{rv} = 26.8 $^m/_s$ and t_f = 10 sec), the required rated motor power P_m is dependant on the ratio of v_{rm} and v_{rv} (Figure 3 and Table 3):

Table 3: Power Requirement as a Function of the Constant Power Range Ratio

	Extended Constant Power Range							
	1:1	1:2	1:3	1:4	1:5	1:6	1:7	1:8
Motor Power (kW)	110	94	74	67	64	62	61	60.6

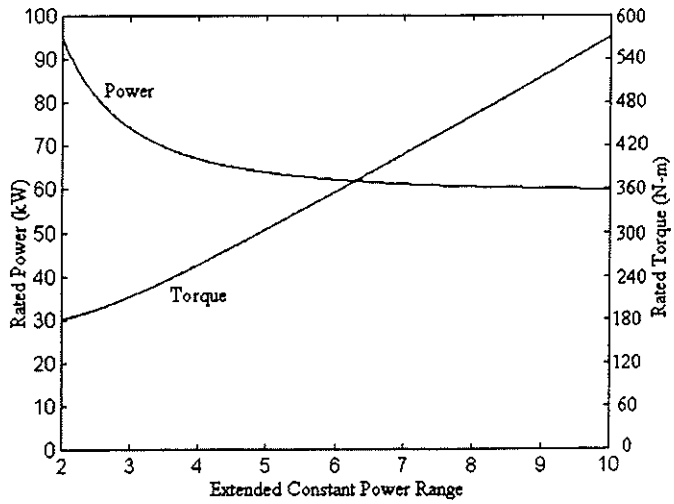

Figure 3. Rated Power and Torque vs. Extended Constant Power Range

Notice that the required torque ratings of extended constant power range motors must be significantly higher, but the required power is lower. After a ratio of about 1:4, the benefit of getting to use a lower power motor begins to become less significant.

PERFORMANCE ANAYLSIS

As shown in Table 3, the required power to reach velocity v_{rv} in time t_f is dependent on the ratio of the constant torque region and the constant power region of the electric motor. Even though the vehicle will reach v_{rv} in time t_f in each case, the nature of the acceleration is variable.

To compute a time t_a for an acceleration to an arbitrary speed v_a while operating in the constant torque region,

$$t_a = \int_0^{V_a} \frac{m \cdot \delta}{F_m - f_{ro} - j_t} \cdot dV \qquad \text{(Eq. 9)}$$

where F_m is the force from the electric motor, f_{ro} is the rolling resistance force (Eq. 2) and f is the areodynamic losses (Eq. 3). Headwinds and climbing resistance are assumed to be negligible in this example, but can easily be added in.

$$t_a = \int_0^{Va} \frac{m \cdot \delta}{\frac{T_{rm} \cdot i_t \cdot \eta_e}{r} - m \cdot g \cdot f_r - \frac{1}{2} \cdot \rho_e \cdot C_D \cdot A_f \cdot V^2} \cdot dV$$

where T_{rm} is the rated torque, i_t is the gear ratio between the motor and the driveshaft, and r is the wheel radius. η_e is the speed of the motor, which is dependent on the instantaneous velocity of the vehicle:

$$\eta_e = \frac{60 \cdot V \cdot i_t}{2 \cdot \pi \cdot r} \qquad \text{(Eq. 11)}$$

To compute the distance S_a covered during this acceleration,

$$S_a = \int_0^{Va} \frac{m \cdot \delta \cdot V}{\frac{T_{rm} \cdot i_t \cdot \eta_e}{r} - m \cdot g \cdot f_r - \frac{1}{2} \cdot \rho_e \cdot C_D \cdot A_f \cdot V^2} \cdot dV$$

To compute the time t_b to accelerate from the rated speed of the motor v_{rm} to any greater speed v_b in the constant power region of operation,

$$t_b = \int_{Vrm}^{Vb} \frac{m \cdot \delta}{\frac{P_m \cdot i_t}{r} - m \cdot g \cdot f_r - \frac{1}{2} \cdot \rho_e \cdot C_D \cdot A_f \cdot V^2} \cdot dV$$

where P_m is the rated power of the motor. Distance can be computed with an equation similar to the constant torque case. Now, by varying the ratio between the constant torque region and the constant power region but keeping the same 0-60mph acceleration in 10 seconds, the acceleration profiles can be seen (Figure 4):

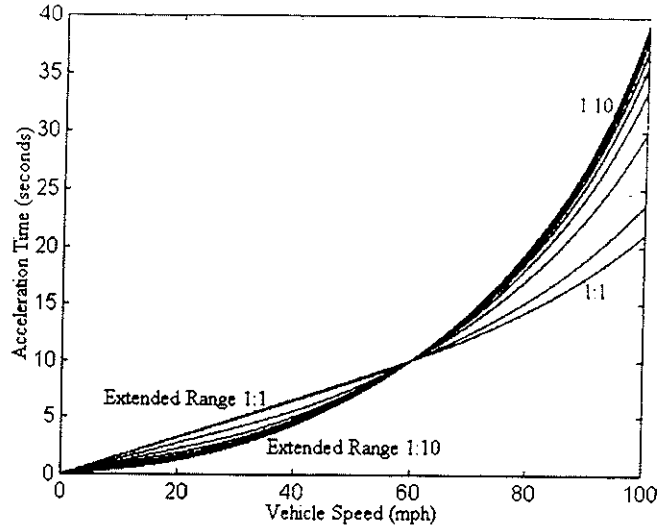

Figure 4. Acceleration Profiles for Different Ratios

Notice that all motors will accelerate to 60 mph in the 10 Seconds but the acceleration curves are different. The extended speed range motors accelerate much more quickly in the beginning and then the acceleration becomes slower at higher speeds. This uneven acceleration affects the distance covered (Figure 5):

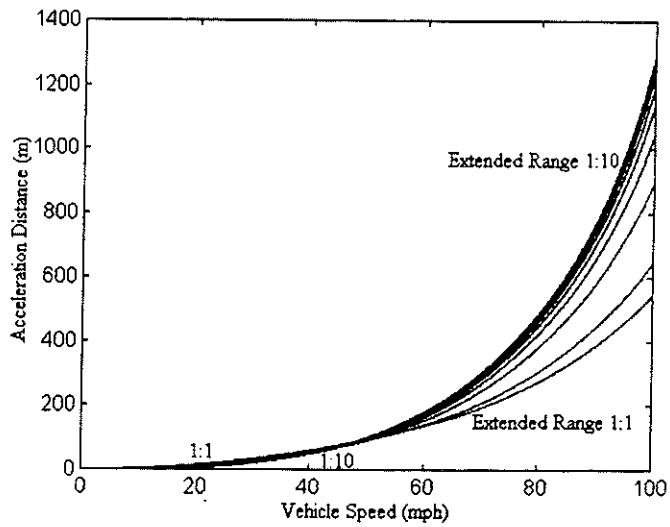

Figure 5. Distance Covered

Notice that vehicles with very low extended constant power ranges (which requires a higher P_m according to Table 3) accelerate to 60 mph in the 10 Seconds but in less distance. This affects passing performance significantly (Figure 6):

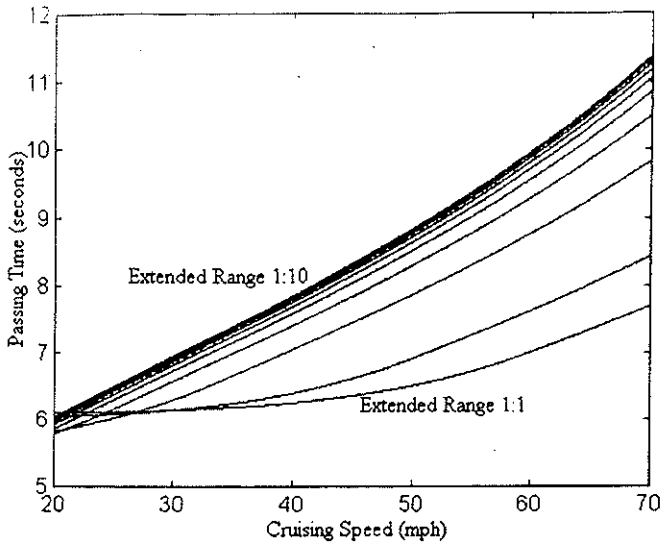

Figure 6. Passing Times

The motors with longer constant power range perform better (shorter passing time) at lower speeds (20 mph), however, the higher power motors (shorter constant power range) perform better at higher speeds. The total distances covered during passing are shown in Figure 7:

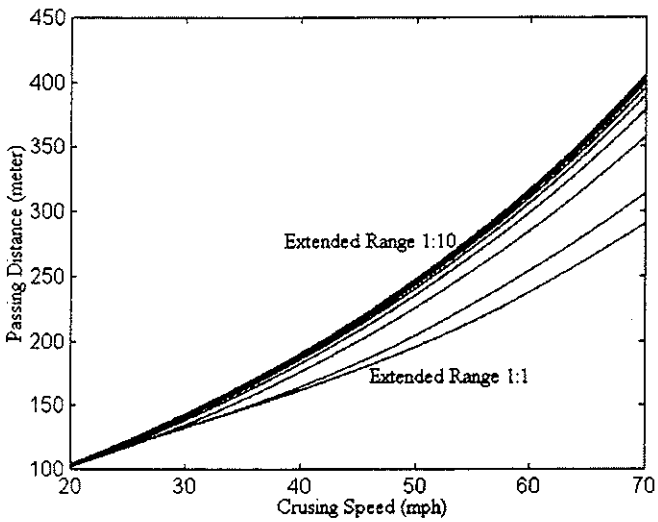

Figure 7. Passing Distance

CONCLUSION

In summary, for simple EV or series HEV designs,

- The power requirement for acceleration decreases as constant power region ratio increases. This results in a smaller motor controller.
- Conversely, the torque requirement for acceleration increases as the constant power region ratio increases. This results in a larger motor size and volume.
- Passing performance suffers considerably as the constant power region ratio increases.

A motor's maximum speed has a pronounced effect on the required torque of the motor. Low speed motors with extended constant power speed range have a much higher rated shaft torque. Consequently, they need more iron and copper to support this higher flux and torque. As motor power decreases (due to extending the range of constant power operation), the required torque is increasing. Therefore, although the converter power requirement (hence the converter cost) will decrease when increasing the constant power range, the motor size, volume, and cost will increase. Increasing the maximum speed of the motor can reduce the motor size by allowing gearing to increase shaft torque. However, the motor maximum speed can not be increased indefinitely without incurring more cost and transmission requirements. Thus there is a multitude of system level conflicts when extending the constant power range.

Several candidate motor technologies were discussed for EV or HEV applications, the induction motor, the brushless DC motor (BLDC) and the switched reluctance motor (SRM). The induction motor has a clear advantage of achieving very high constant power range ratios, but suffers by requiring a very high torque rating. The relatively low maximum speed of the induction motor compounds this problem, because the motor cannot be geared down to the driveshaft an appreciable amount.

The SRM achieves a balance of a modest extended constant power range and a very high maximum speed. Extending the constant power range beyond what the SRM offers yields very little additional benefits (Table 3 and Figure 3). The high maximum speed allows for the SRM to be geared at twice the gear ratio of the induction or BLDC motors, halving the required maximum torque.

The examples presented in this paper form a methodology for evaluating tradeoffs between the power requirement, torque requirement, acceleration performance, and passing performance for different motor technologies. Initial studies indicate that the switched reluctance motor is a good candidate by achieving an optimal balance of these criteria. The same evaluation techniques can be implemented on more complex designs, including parallel or series-parallel type hybrid electric vehicles.

CONTACT

Stephen Moore and Dr. Mehrdad Ehsani can be reached by calling the Department of Electrical Engineering, Texas A&M University, at (409) 845-7441, or email smoore@ee.tamu.edu and ehsani@ee.tamu.edu.

REFERENCES

[1] C. C. Chan, and K. T. Chau, "Advanced ac propulsion systems for electric vehicles," in *Proc. Int. Symp.*

Automotive Technology Automation, 1991, pp. 119-125.

[2] J. L. Oldenkamp, and S. C. Peak, "Selection and design of an inverter-driven induction motor for a traction drive system," *IEEE Trans. on Industry Applications*, Vol. IAS-21, No. 1, Jan./Feb., 1985, pp. 259-265.

[3] C. C. Chan, J. Z. Jiang, G. H. Chen, and K. T. Chau, "Computer simulation and analysis of a new polyphase multipole motor drive," *IEEE Trans. Industrial Electronics*, Vol. 40, 1993, pp. 570-576.

[4] C. C. Chan, W. S. Leung, and K. T. Chau, "A new permanent magnet motor drive for mini electric vehicle," in *Proc. Int. Electric Vehicle Symp.*, 1990, pp. 165-174.

[5] C. C. Chan, J. Z. Jiang, G. H. Chen, X. Y. wang, and K. T. Chau, "A novel polyphase multipole square wave permanent magnet motor drive for electric vehicle," *IEEE Trans. Industry Applications*, 1994, pp. 1258-1266.

[6] T. J. E. Miller, *Brushless Permanent Magnet and Reluctance Motor Drives*, London, U.K., Oxford Univ. Press, 1989.

[7] W. L. Soong and T. J. E. Miller, "Field weakening performance of brushless synchronous AC motor drives," *IEE Proc.-Electr. Power Appl.*, Vol. 141, No. 6, pp. 331-340, November 1994.

[8] P. J. Blake, R. M. Davis, W. F. Ray, N. N. Fulton, P. J. Lawrenson, and J. M. Stefenson, "The control of switched reluctance motors for battery electric road vehicles," *International Conference on PEVD*, pp. 361-364, May, 1984.

[9] Automotive Handbook, Germany: Robert Bosch Gmbh, 1986.

99P-220

A Charge Sustaining Parallel HEV Application of the Transmotor

Stephen W. Moore
Texas A&M University

Mehrdad Ehsani
Texas A&M University

ABSTRACT

An electromechanical gear is presented along with design examples utilizing the electromechanical gear in hybrid electric vehicle drive trains. The designs feature the electromechanical gear (the Transmotor) in place of traditional mechanical transmissions and/or gearing mechanisms. The transmotor is an electric motor suspended by its shafts, in which both the stator and the rotor are allowed to rotate freely. The motor thus can provide positive or negative rotational energy to its shafts by either consuming or generating electrical energy.

A design example is included in which the transmotor is installed on the output shaft of an internal combustion engine. In this arrangement the transmotor can either increase or decrease shaft speed by applying or generating electrical power, allowing the ICE to operate with a constant speed. A torque splitting device is then employed to absorb excess torque produced by the engine or to create supplementary torque when needed, allowing the ICE to operate with constant torque. Thus a constant speed constant torque engine can be directly coupled to the output drive shaft by using electric machines.

The governing equations, a control strategy and an analysis corresponding to each operating mode of the architecture are presented. The operating regions and boundaries of individual components are investigated and engine, motor and energy storage system sizing are identified.

INTRODUCTION

An ordinary automobile transmission is presently the most common method utilized to match the speed of the powerplant (usually an internal combustion engine) to the speed of the driveshaft [1]. Transmissions face the problem of having to constantly switch gear ratios as the vehicle's speed changes. A type of automobile transmission called the Continuously Variable Transmission (CVT) overcomes the traditional problems of having to switch gears.

The electromagnetic gear offers superior characteristics for the automotive designer over the traditional transmission and the CVT. Both types of mechanical transmissions are a 'two-port' design, meaning that there are two connections, the input shaft and the output shaft. The transmotor is a 'three-port' design, meaning that there are three connections, the input shaft, the output shaft, and an electrical connection. The addition of the extra connection allows for design and operational flexibility over the mechanical designs. This allows the electromagnetic gear to actively generate or absorb electrical or mechanical power, whereas the traditional transmissions only allow the passage of mechanical power.

The electromechanical gear is a rotating electric machine in which both the rotor and the stator are free to rotate [2,3,4], with the electrical energy being delivered with brush or slip ring mechanisms. The machine can operate as either a motor if it converts electrical energy into mechanical energy or as a generator if it converts mechanical energy to electrical energy. Furthermore, depending on the relative speeds of the rotor and stator and the direction of the torque developed on the rotor, the transmotor can operate in all four modes (forward motoring, forward generating, reverse motoring, reverse generating).

THE ELECTROMECHANICAL GEAR

An ordinary electric motor features two connections, one electrical and one mechanical. Ordinary motors can operate in four possible scenarios:

- Output shaft rotating clockwise while providing positive torque (forward motoring),
- Output shaft rotating counterclockwise while providing positive torque (reverse motoring),

- Output shaft rotating clockwise while absorbing torque (forward generating),
- Output shaft rotating counterclockwise while absorbing torque (reverse generating).

In comparison, the electromechanical gear features three connections, the rotor shaft, the stator shaft, and the electrical connection (Figure 1).

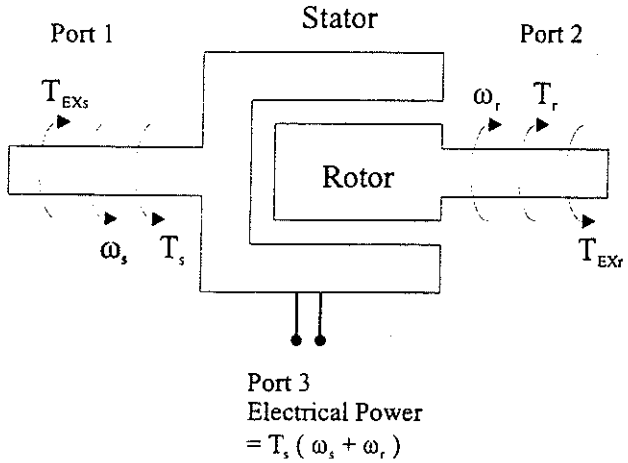

Figure 1. Electromechanical Gear

Where ω_s is the rotational speed of the stator, ω_r is the rotational speed of the rotor and T_{EXs} and T_{EXr} are the external torques applied to the shafts. Since the transmotor is suspended in space, torque is conserved. When torque is produced in the transmotor, it acts equally on the stator and the rotor in opposite directions. In Figure 1 the electromechanical torque developed in the machine is T_r, which acts on the rotor as shown. An equal but opposite torque T_s, acts on the stator. Although the electromechanical torques on the rotor and stator are equal in magnitude, they interact with the externally applied torques T_{EXr} and T_{EXs} to result in different angular speeds for the rotor and stator. Thus in Figure 1, the rotor speed ω_r, and the stator speed ω_s, can be different in magnitude as well as direction. Depending on the relative speed between the rotor and stator and the electromechanical torque developed in the machine, the electromechanical gear can operate in four possible quadrants similar to a traditional electric machine (Figure 2):

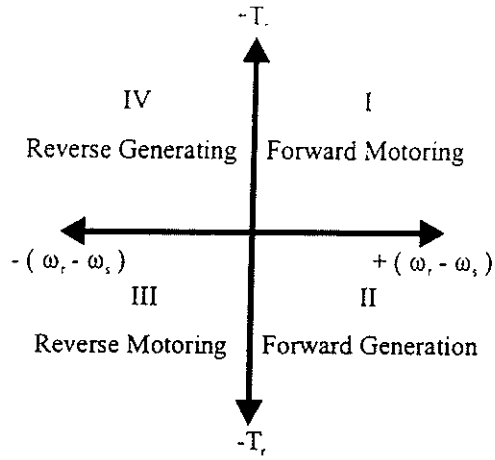

Figure 2. Four Quadrants of Operation

In Figure 1, $T_r = T_s$ and is equal to the electromechanical torque developed in the machine. The stator is assumed to be rotating at speed ω_s, in an opposite direction to the rotor speed ω_r. The law of conservation of energy holds true for any electromechanical system. Applying instantaneous power balance to the electromechanical gear shown in Figure 1:

Electrical Power Input + Mechanical Power Input = Electrical Power Output + Mechanical Power Output

which implies,

Electrical Power at Port 3 = Mechanical Power at Port 1 + Mechanical Power at Port 2

Applying values to these quantities,

Electrical Power $= T_s \omega_s + T_r \omega_r$ (Eq. 1)
Electrical Power $= T_r (\omega_r + \omega_s)$ (since $T_r = T_s$) (Eq. 2)

Thus it is observed that the electrical power input into the electromagnetic gear is split into mechanical power output at the stator and rotor shafts. The four possible operating modes of the machine are shown in Figure 2 and are classified as:

- Quadrant I. Forward motoring
- Quadrant II. Forward generating
- Quadrant III. Reverse motoring
- Quadrant IV. Reverse generating.

In the forward motoring quadrant, the rotor moves in the positive direction with respect to the stator. The electromechanical torque developed on the rotor acts in the positive direction in this mode. In the forward generating quadrant the rotor still moves in the positive direction relative to the stator, but now the electromechanical torque acting on the rotor is in the negative direction. The electromagnetic gear operates in the reverse motoring quadrant when the rotor moves in

the negative direction with respect to the stator, and the electromechanical torque acts in the negative direction on the rotor. In the reverse generating quadrant, the rotor moves in the negative direction relative to the stator, while the electromechanical torque acts in the positive direction on the rotor.

The electromagnetic gear can operate in any one of the four quadrants shown in Figure 2 depending on the relationship between T_r, ω_r, and ω_s. Notice that the clockwise direction of rotation is considered to be positive. Because there are three ports, there are nine possible (3^2) major operating modes consisting of 21 minor modes of operation.

If the stator is held in place (i.e. $\omega_s = 0$) by an infinite external torque T_{Exs}, the transmotor performs like an ordinary electric machine. The rotor will spin at the speed ω_r and produce torque T_r. It will operate in all four quadrants in this manner. The same holds true if the rotor is held fixed ($\omega_s = 0$) by an external torque T_{Exr}. Then the stator will spin at the speed ω_s and produce torque T_s. The electrical power consumed would be T_s ω_s.

If the stator and rotor speeds are exactly matched ($\omega_s = \omega_r$) then the motor will simply rotate in place producing nor consuming any torque or electrical energy. It is in this mode that the transmotor can perform as an electrical clutch, because the external torques applied to the motor can not exceed the transmotor's torque rating without slipping. By varying the transmotor's magnetic field, the torque threshold can be adjusted.

If the stator and the rotor are spinning in the same direction but one is faster than the other, the transmotor operates in all four quadrants depending on the applied and produced torques. For example, consider the transmotor stator attached to an ICE producing T_{EXs} torque and spinning at speed ω_s (Figure 3). If the driveshaft is at zero speed ($\omega_r = 0$) then the transmotor is *generating* electrical power (Quadrant III). If the vehicle is traveling at high speeds and the rotor speed is faster than the stator speed ($\omega_r > \omega_s$) then the transmotor is *consuming* electrical power (Quadrant I). In both scenarios, the transmotor does not contribute torque, and the torque applied to the driveshaft is T_{EXs}. Similar scenarios take place under regenerative braking.

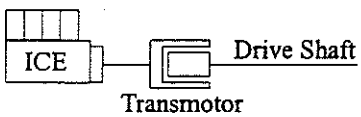

Figure 3. Simple Application of the Transmotor

The closest mechanical system to the transmotor is the planetary gear. A planetary gear has three mechanical ports as does the transmotor (Figure 4):

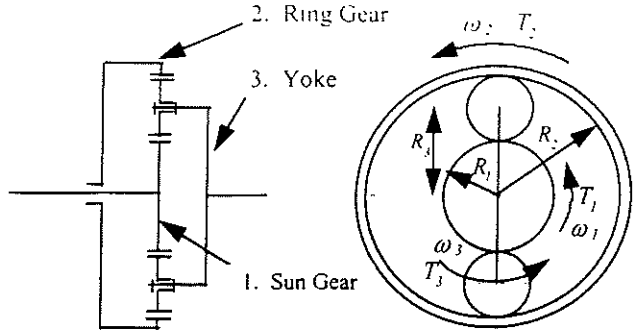

Figure 4. Planetary Gear

There are three major components of the planetary gear, the sun gear (1), the ring gear (2), and the yoke (3). The torque and speed relationships for the planetary gear are:

$$\omega_3 = \frac{R_1}{2R_3}\omega_1 + \frac{R_2}{2R_3}\omega_2 \qquad \text{(Eq. 3)}$$

$$T_3 = \frac{2R_3}{R_1}T_1 = \frac{2R_3}{R_2}T_2 \qquad \text{(Eq. 4)}$$

where R_1, R_2 and R_3 are the radii of the different gears. Ignoring the effects of gear sizing, the fundamental operation of the planetary gear system is:

$$\omega_3 \approx \omega_1 + \omega_2 \qquad \text{(Eq. 5)}$$

$$T_3 \approx T_1 \approx T_2 \qquad \text{(Eq. 6)}$$

These equations state that when torque is applied on two of the ports, the third port must also have that same torque (or a factor of those torques when given gear sizing). They also state that when speeds are applied to two ports, the third port will display a sum of those speeds. These equations compare with the transmotor governing equations:

$$\omega_r = \omega_s + \omega_e \qquad \text{(Eq. 7)}$$

$$T_r = T_s \qquad \text{(Eq. 8)}$$

where ω_e is the speed produced by the electrical port. Notice that these equations are a dual of the planetary gear equations. Attaching an electric motor to one of the planetary gear ports, a transmotor equivalent can be made (Figure 5):

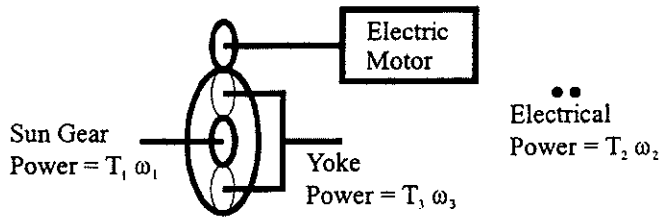

Figure 5. Transmotor Equivalent

Notice that this duality does not take into account the torque and speed translations due to the differing radii of the planetary gears.

EXAMPLE HYBRID ARCHITECTURES

There are almost an unlimited ways in which electric motors, gears, engines, and other drivetrain components can be arranged into vehicle powertrains. This section will describe a few example architectures featuring the transmotor. First, the basic hybrid architectures are presented:

- Series Hybrid

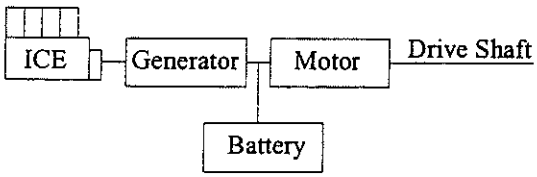

Figure 6. Series Hybrid

The series hybrid is much like an electric vehicle with the exception of on-board electricity generation [5]. The ICE and generator produce the average energy requirement of the vehicle and additional transient power is provided by the battery pack. A series hybrid is not limited to ICE and generator. Many options exists such as fuel cells, thermoelectric cells, and turbine generators.

- Parallel Torque Summing Hybrid

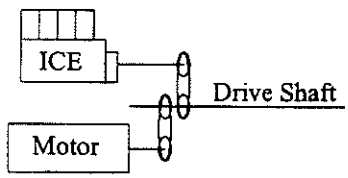

Figure 7. Parallel Torque Summing Hybrid

The torque summing hybrid uses a drive shaft with belts [6] or gears to combine the torques of the ICE and electric machine. The torque summing hybrid can operate in two basic modes. When the ICE torque is too low, the electric machine can add power to the driveshaft by increasing the torque. When the ICE torque is more than the vehicle demand, the electric machine can absorb energy from the driveshaft by producing electricity. More modes of operation can be created by the addition of clutches, transmissions, and electromagnetic locks, but the two basic modes of operation remain the same. A pass-though type motor can be used in place of the belt or gear torque summing device [7,8,9,10,11]:

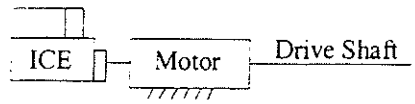

Figure 8. Torque Summing Hybrid

A Torque summing hybrid allows the ICE to be sized smaller than the peak torque demand of the vehicle, however, the ICE is forced to operate over its entire torque and speed ranges. In this case, the ICE is sized for the average torque and the electric motor sized for the peak torque requirement. A version of this design is also known as the Petro Electric Drivetrain [12].

- Parallel Speed Summing Hybrid

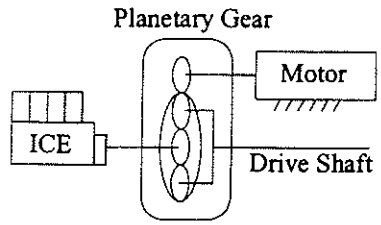

Figure 9. Speed Summing Hybrid

This speed summing hybrid uses a planetary gear system to combine the speeds of the ICE and electric machine. The electric machine cannot contribute or subtract torque from the system, only rotational speeds. With the transmotor, the planetary gear system can be removed:

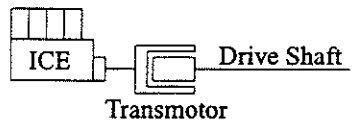

Figure 10. Simplified Speed Summing Hybrid

The speed summing hybrid has two basic modes. When the ICE's speed is too low, the electric machine can add power to the driveshaft by increasing rotational speed. When the ICE is operating too fast, the electric machine can absorb rotational energy from the driveshaft by generating electricity. More modes of operation can be created by the addition of clutches and locks, but the two basic modes remain the same. Notice the ICE can operate at a single speed in this configuration, but must vary its torque production.

- Parallel Speed Summing Hybrid with Transient Torque Sink

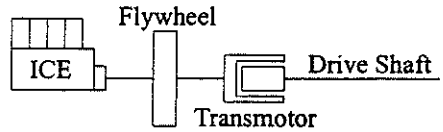

Figure 11. Speed Summing with Torque Sink

The addition of the flywheel provides the transmotor with a transient torque sink in which it can act against to add torque to the driveshaft. This allows for the ICE to be sized smaller than the peak required torque because transient torque can be obtained from the flywheel's rotational energy. However, the torque sink is limited and gradability and load carrying capability is limited to ICE sizing.

- Series/Parallel Hybrid

The disadvantages of a parallel torque summing hybrid vehicle are substantial. The ICE is not operated strictly in its peak efficiency region, but instead its operation varies as a function of vehicle speed. The electric machine in the torque summing hybrid is the primary torque device, providing transient and peak power. The engine serves as a secondary torque device and average power source. The inverse of these properties are true with a speed summing hybrid. The ICE is allowed to operate at an optimal speed, but the torque output is variable, forcing the engine to operate outside of its peak efficiency region. The engine in this case is the only torque device, thus forcing the designer to match the ICE to the torque demands of the vehicle. These disadvantages are eliminated with the series hybrid architecture. The ICE is coupled directly to a generator and operated at an optimal speed and torque. Thus the ICE does not contribute power directly to the vehicle drive shaft. This arrangement puts the full burden of powering the vehicle on the propulsion motor(s). Series hybrids tend to be costly due to the large generator and propulsion motor sizes.

A possible hybrid design methodology to allow the ICE to operate at a constant optimal torque and speed is to combine the parallel and series architectures:

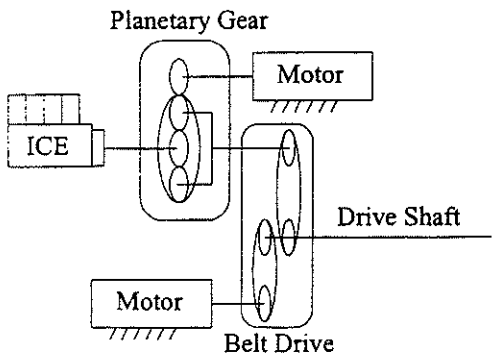

Figure 12. Series/Parallel Hybrid

This series/parallel hybrid architecture has been demonstrated roughly in the Toyota Prius, the first mass-produced hybrid electric vehicle. There are several other combinations of series/parallel designs [13]. The architecture is capable of four basic modes of operation with the ICE operating at a constant torque and RPM:

1. Slow vehicle speed and accelerating. The planetary gear/motor subtracts speed from the ICE by generating electricity to match its speed to the driveshaft speed. The driveshaft motor adds extra torque for acceleration.
2. Slow speeds decelerating. The planetary gear subtracts speed from the ICE shaft and the driveshaft motor subtracts torque from the driveshaft by generating electricity.
3. Fast vehicle speed and accelerating. The planetary gear motor supplements the ICE speed and the driveshaft motor adds extra torque for acceleration.
4. Fast speeds decelerating. The planetary gear adds speed to the ICE shaft and the driveshaft motor subtracts torque.

Additional modes are available as well:

5. Electric mode only. In this mode, the driveshaft motor provides all the power required by the vehicle.
6. Series mode only. The planetary gear consumes all available power from the ICE to charge the batteries. The driveshaft motor provides all traction power requirements.

The series/parallel architecture can be improved upon by the use of a transmotor:

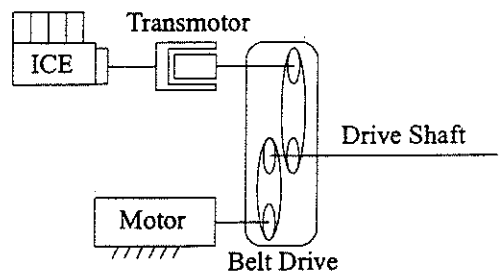

Figure 13. Transmotor Application

This arrangement removes the necessity of the planetary gear system, thus improving the mechanical efficiency of the system. However, the mechanical torque summing device (gears, belts, ect.) still imposes design and efficiency penalties. The torque summing device can be replaced with an in-line motor mounted in series with the transmotor:

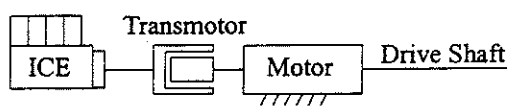

Figure 14. Simplified Series/Parallel Architecture

This architecture has four basic modes of operation similar to the four listed previously. In addition, there are five other significant modes:

5. Cruise. The transmotor matches the ICE speed to the driveshaft (consumes electrical power) and the in-line motor absorbs excess torque from the ICE (generates electrical power), resulting in a net electrical energy flow of zero.
6. Charging Cruise. The ICE operates outside of its optimal region to produce excess RPM and torque, which is converted to electrocute by the motors.
7. Engine Mode. The ICE operates with variable speed and torque, thus minimizing the work required by the electric motors.
8. EV Only Mode (requires a lock or clutch). The shaft of the ICE is locked in place and the motors are used in series are a primary mover, powered by the battery pack.
9. Standstill Charging. The transmotor absorbs all energy from the ICE to charge the battery and the in-line motor is used to lock the driveshaft.

Major design obstacles for the implementation of the transmotor in this architecture are not trivial. The foremost concern is the requirement for two motors and two motor controllers, which results in an increase of system cost. However, this penalty is reduced slightly because each motor and controller does not have to carry the full propulsion load of the vehicle and can be sized smaller. Initial simulations suggest that although the transmotor has to be rated for the full torque of the ICE, its rated power can be a third of the rated power of the traction motor.

Other design considerations involve the actual construction of the transmotor unit. Because the transmotor floats on its shafts, it presents a challenge to deliver the electrical power to the stator and rotor. The bearings and mechanical support for the motor are also an issue.

Since the transmotor and traction motor are configured to be in series with this design, it is plausible that the stator of the transmotor be extended outwardly and serve as a flywheel. An addition of a flywheel to the series/parallel architecture would create an additional torque sink, allowing smaller component sizing.

CONCLUSION

The transmotor is an electric motor suspended by its shafts, in which both the stator and the rotor are allowed to rotate freely. Electric power is supplied to the rotor or stator (or a combination of the two, depending on the motor technology implemented) using a delivery mechanism such as slip-rings. In this manner, the transmotor can be used to consume or generate electrical power given a rotational speed differential between the rotor and the stator. Because the transmotor is suspended, it cannot contribute a torque component (positive or negative) to the driveshaft.

The transmotor can operate in all four quadrants: forward motoring, forward generating, reverse motoring, and reverse generating like an ordinary electric machine. In addition, these four modes can be broken down into 21 minor modes, which allows the hybrid designer a high degree of flexibility in his control scheme.

The transmotor's speed summing property makes it an ideal active replacement for traditional mechanical transmissions. Traditional transmissions are a 'two-port' design, meaning that there are two connections, the input shaft and the output shaft. The transmotor is a 'three-port' design, meaning that there are three connections, the input shaft, the output shaft, and an electrical connection. The addition of the extra connection allows for design and operational flexibility over the mechanical designs.

Many modern hybrid architectures feature planetary gears as speed summing devices to match the output speed of an ICE to the rotational speed of the driveshaft. The transmotor is the electromechanical dual of the planetary gear system.

Design obstacles facing hybrid designers wanting to implement speed summing parallel hybrid topologies

CONTACT

Stephen Moore and Dr. Mehrdad Ehsani can be reached by calling the Department of Electrical Engineering, Texas A&M University, at (409) 845-7441, or email smoore@ee.tamu.edu and ehsani@ee.tamu.edu.

REFERENCES

1. Davis, Gregory W., "The Development of an Electo-Hydraulically Controlled, Five-Speed Transmission for a Hybrid Electric Vehicle," SAE Paper No. 980830.
2. Sodhi, Sameer, "Electromagnetic Gearing Applications in Hybrid Electric Vehicles," Ph.D. Dissertation, Texas A&M University, August, 1994.
3. Wakefield, E. H., "History of the Electric Automobile," SAE Publication, 1994.
4. Weisenburger, G.E., "Electric Motor", U.S. Patent #667,275, Filed Feb. 1900.
5. A. F. Burke, "Hybrid/electric vehicle design options and evaluations," *SAE Journal Publications,* Paper No. 920447, Feb., 1992.
6. Johnston, B., et al, "The Continued Design and Development of the University of California, Davis Future Car," SAW Paper 980487.
7. Ehsani, M., K.M. Rahman, and H.A. Toliyat, "Propulsion System Design of Electric and Hybrid Vehicles," IEEE Transaction of Industrial Electronics.
8. Toliyat, H.A., K.M. Rahman, and M. Ehsani, "Electric Machine in Electric and Hybrid Applications," Proceedings of ICPE, 1995, Seoul, pp. 627-635.
9. Ehsani, M., "Electrically Peaking Hybrid System and Method," U.S. Patent granted, 1996.
10. Howze, J., M. Ehsani, and D. Buntin, "Optimizing Torque Controller for a Parallel Hybrid Electric Vehicle," U.S. Patent granted, 1996.
11. Gao, Yimin, K. Rahman, and M. Ehsani, "Parametric Design of the Drive Train or an Electrically Peaking Hybrid (ELPH) Vehicle," ASE paper 970294.
12. Jeffries, P.N. and A.E. Corbett, "The Petro-Electric Drivetrain," IEEE Colloquium on Motors and Drives for Battery Powered Propulsion, digest no. 080, pp. 7/1-4, Apr. 1993.

13. Willis, F.G., and R.R. Radtke, "Hybrid Vehicle System Analysis," SAE paper 920447.

A Matlab-based Modeling and Simulation Package for Electric and Hybrid Electric Vehicles Design

Karen Butler, *Member,IEEE*, Mehrdad Ehsani, *Fellow,IEEE*, Preyas Kamath, *Student Member,IEEE*

Abstract **- This paper discusses a simulation and modeling package developed at Texas A&M University, V-Elph 2.01. V-Elph facilitates in-depth studies of electric (EV) and hybrid electric (HEV) vehicle configurations or energy management strategies through visual programming and by creating components as hierarchical subsystems which can be used interchangeably as embedded systems. V-Elph is composed of detailed models of four major types of components: electric motors, internal combustion engines, batteries, and support components which can be integrated to model and simulate drive trains having all electric, series hybrid, and parallel hybrid configurations. V-Elph was written in the Matlab/Simulink graphical simulation language and is portable to most computer platforms.**

This paper also discusses the methodology for designing system level vehicles using the V-Elph package. An EV, a series HEV, a parallel EV, and a conventional ICE driven drive train have been designed using the simulation package. The simulation results such as fuel consumption, vehicle emissions, and complexity are compared and discussed for each vehicle.

I. INTRODUCTION

Presently, only electric and low-emissions hybrid vehicles can meet the criteria outlined in the California Air Regulatory Board (CARB) regulations which require a progressively increasing percentage of automobiles to be ultra-low or zero emissions beginning in the year 1998 [1]. Though purely electric vehicles are a promising technology for the long range goal of energy efficiency and reduced atmospheric pollution, their limited range and lack of supporting infrastructure may hinder their public acceptance [2]. Hybrid vehicles offer the promise of higher energy efficiency and reduced emissions when compared with conventional automobiles, but they can also be designed to overcome the range limitations inherent in a purely electric automobile by utilizing two distinct energy sources to provide energy for propulsion. With hybrid vehicles, energy is stored as a petroleum fuel and in an electrical storage device such as a battery pack and is then converted to mechanical energy by an internal combustion engine (ICE) and electric motor, respectively. The electric motor is used to improve energy efficiency and vehicle emissions while the ICE provides extended range capability. Though many different arrangements of power sources and converters are possible in a hybrid power plant, the two generally accepted classifications are series and parallel [3].

Computer modeling and simulation can be used to reduce the expense and length of the design cycle of hybrid vehicles by testing configurations and energy management strategies before prototype construction begins. Interest in hybrid vehicle simulation began to pick up in the 1970's along side the development of several prototypes which were used to collect a considerable amount of test data on the performance of hybrid drive trains [4]. Also studies have been conducted to study the hybrid electric vehicle concepts [5-7]. Several computer programs have since been developed to describe the operation of hybrid electric power trains, including: Simple Electric Vehicle Simulation (SIMPLEV) from the DOE's Idaho National Laboratory [8], MARVEL from Argonne National Laboratory [9], CarSim from AeroVironment Inc., JANUS from Durham University [10], and ADVISOR from the DOE's National Renewable Energy Laboratory [11]. A previous simulation model, ELPH, developed at Texas A&M University was used to study the viability of an electrically-peaking control scheme and to determine the applicability of computer modeling to hybrid vehicle design [12] but was essentially limited to a single vehicle architecture. Other work conducted by the hybrid vehicle design team at Texas A&M University is reported in [13-17].

V-Elph [18-19] is a system level modeling, simulation and analysis package developed at Texas A&M University using Matlab/Simulink [20] to study issues related to electric vehicle (EV) and hybrid electric vehicle (HEV) design such as energy efficiency, fuel economy, and vehicle emissions. V-Elph facilitates in-depth studies of power plant configurations, component sizing, energy management strategies, and the optimization of important component parameters for any type of hybrid or electric configuration or energy management strategy. It uses visual programming techniques, allowing the user to quickly change architectures, parameters, and to view output data graphically. It also includes detailed models of electric motors, internal combustion engines, and batteries developed at Texas A&M University.

This paper discusses the methodology for designing system level vehicles using the V-Elph package. An EV, a series HEV, a parallel EV, and a conventional ICE driven drive train have been designed using the simulation package. The simulation results are compared and discussed for each vehicle.

II. Drive Train Design Methodology

Several levels of depth are available in V-Elph to allow users to take advantage of the features that interest them. At the most basic level, a user can run simulation studies by selecting one of the electric vehicles, series or parallel hybrid vehicles, or conventional vehicles provided and display the results using the graphical plotting tools. In addition to being able to change the drive cycle and the environmental conditions under which the vehicle operates, the user can switch components in and out of a vehicle model to try different types of engines, motors, and batteries models. The user can also change vehicle characteristics such as size and weight, gear ratios, and the size of the components that make up the drive train.

An intermediate user can create his/her own vehicle configurations using a blank vehicle drive train template as shown in fig. 1. This drive train was constructed graphically by connecting the main component blocks (drive cycle, controller, power plant, vehicle dynamics) using the Simulink visual programming methodology through the connection of the appropriate input and output ports. The power plant is blank and is designed using component models selected from a component library. Components can be isolated to run parameter sweeps that create performance maps which assist in component sizing and selection. A controller block is designed with logic statements which create the signals required to control the individual system-level components. A vehicle dynamics block is designed with input parameters such as road angle, mass, and drag coefficient necessary to compute vehicle output dynamic parameters such as engine speed and road speed. The drive cycle block is designed by selecting a drive cycle from those supplied by the package or creating a new drive cycle.

Finally, advanced users can pursue sophisticated design objectives such as the creation of entirely new component models and the optimization of a power plant by creating add-on features that are compatible with the modeling system interface.

V-Elph allows the interconnection of virtually any type of electrical or mechanical component utilized in a vehicle drive train, even experimental technologies such as ultra-capacitors. Component models can be created from look-up tables, empirical equations, and both steady-state and dynamic equations. Each component model is created from the general model and interface shown in fig. 2. The component models are stored in a library, called the library of components as shown in fig. 3. The speed at which the simulation executes is highly dependent on the complexity of the component models used in a vehicle design. The various detailed component models currently utilized in the V-Elph package were developed by members of the ELPH research team at Texas A&M University.

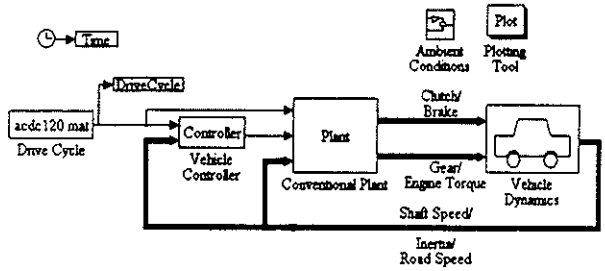

Fig. 1. System level representation of a general vehicle drive train in V-Elph

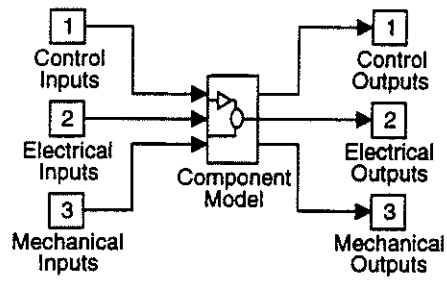

Fig. 2 Component Input/Output interface

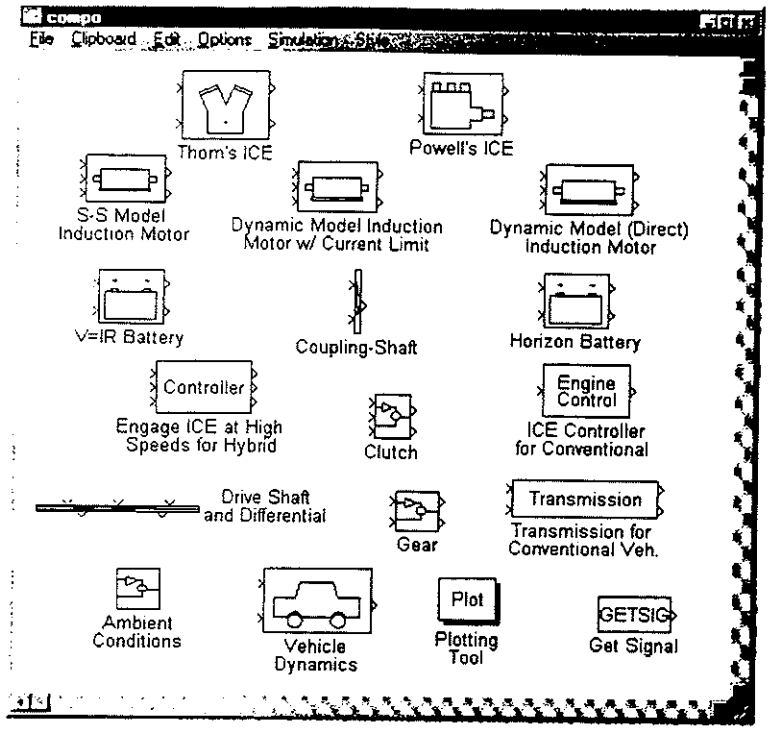

Fig. 3. Library of Components

I. DESIGN OF VEHICLE DRIVE TRAINS

In this section, the design and analysis of an electric vehicle drive train, two parallel hybrid vehicle drive trains with different control strategies, a series hybrid electric vehicle drive train, and a conventional internal-combustion-engine-driven vehicle drive train using the V-Elph package are discussed. A description is given of the performance specifications and the control strategy and power plant developed for each vehicle design. A typical mid-sized family sedan was used as the basis for each vehicle. The vehicles' components were sized to provide enough power to maintain a cruising speed of 120 km/h on a level road and acceptable acceleration performance of 0 to 100 km/h in 16 seconds for short time intervals. The vehicles were also designed to maintain highway speeds for an extended period of time and provide adequate performance on hills. The same ICE, motor, battery, and vehicle dynamics models were used for each vehicle design with appropriate changes made to the model parameters to meet the specific vehicle performance requirements.

Simulation studies were performed for each vehicle using a simple acceleration and deceleration drive cycle, an FTP-75 urban drive cycle, a federal highway drive cycle, and a commuter drive cycle. Various performance parameters generated during the simulation studies are graphically presented in the paper. Also a table is included which compares such performance parameters as fuel consumption and emissions for each simulation study.

A. ICE Conventional Drive Train Design

The conventional ICE-driven drive train was designed based on the specifications of a Buick LeSabre ('91 model) [21]. The vehicle's 4-speed automatic transmission was modeled as a manual transmission with a clutch, retaining the same overall gear ratios. It is a 4 door sedan, 6 passengers vehicle with a desired 0-60 mph in the 10 seconds range characteristic and a curb weight of 3483 lbs (1580 kgs). The power plant is shown in fig. 4. Table 1 shows the engine and vehicle specifications utilized to design the conventional drive train.

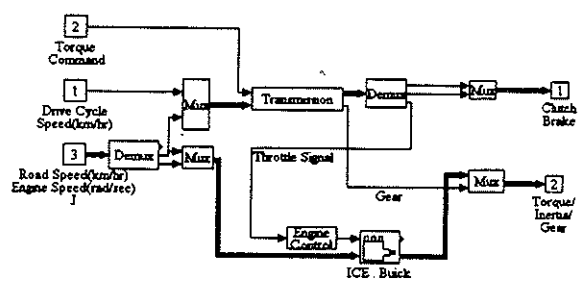

Fig. 4. Power plant representation of conventional vehicle drive train designed using V-Elph

TABLE I.
SPECIFICATIONS OF ICE DRIVE TRAIN

Engine Specifications			
Total Displacement		3.791 liter	
Max Torque		298 Nm at 3200 rpm	
Max Power		125 KW at 4800 rpm	
Vehicle Specifications			
Curb Weight		1580 kg	
Acceleration		0-60 mph in 10 s	
Overall Gear Ratios			
1st	2nd	3rd	4th
8.94	4.804	3.06	2.142

A. *Parallel Hybrid Electric Drive Train Design*

In a typical parallel design, consisting of an ICE and an electric motor in a torque-combining configuration, either the ICE or the electric motor can be considered the primary energy source depending on the vehicle design and energy management strategy. Also the drive train can be designed such that the ICE and electric motor are both responsible for propulsion or each is the prime mover at a certain time in the drive cycle. A component's functional role could change within the course of a drive cycle due to battery depletion or other vehicle requirements. Vehicle architecture decisions, control strategies, component selection and sizing, gearing, and other design parameters become considerably more complex in a parallel hybrid due to the sheer number of choices and their effect on a vehicle's performance given a particular mission.

The vehicle drive train configuration in fig. 5 was designed in V-Elph for a parallel HEV. It is based on a typical mid-sized family sedan with a gross mass of 1838 Kg that includes the additional batteries used in the hybrid power plant. The drive train includes a controller which manipulates the torque contributions of the electric motor and ICE. The battery provides power for the induction motor. The ICE model was sized to provide enough power to maintain a cruising speed of 120 km/h on a level road and the electric machine was sized to provide acceptable acceleration performance of 0 to 100 km/h in 16 seconds for short time intervals.

The ICE model was designed based on Powell's engine analysis [22]. The induction machine model [13] performs two functions in the drive train; as a motor it provides torque at the wheels to accelerate the vehicle and as a generator it recharges the battery during deceleration (regenerative braking) or whenever the torque produced by the power plant exceeds the demand from the driver. Vector control was utilized to extend the constant power region of the motor, making it possible to run the motor over a wide speed range. The motor can provide the requested torque up to the constant power threshold at speeds above the base speed of the motor; operation beyond this point is restricted to avoid exceeding the motor's power rating. The HEV design utilizes the wide speed range of the vector controlled induction motor to improve the overall system efficiency.

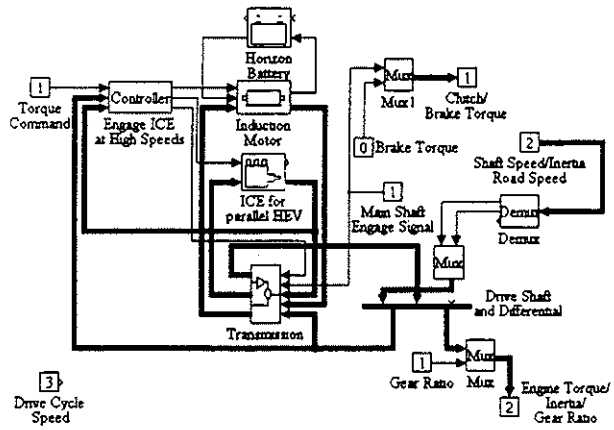

Fig. 5. Parallel HEV drive train configuration

The battery model [23] uses the current load and battery state of charge to determine dc bus voltage. Voltage tends to drop as the state of charge decreases and as the amount of current drawn from the battery increases. At low currents, the battery efficiency is reasonably high regardless of the state of charge. As the amount of current drawn from the pack increases, the battery efficiency drops rapidly to about 75% for a 400 A drain. At current levels up to about 100 A the battery recharge efficiency is relatively high but quickly drops off above this threshold because the physical and chemical processes in the battery can not react quickly enough to absorb the energy, resulting in battery degradation. It is thus desirable to perform battery charging at current levels of 100 A or less whenever possible.

Two parallel HEV drive trains were designed using a different control strategy, referred to as control strategy 1 and control strategy 2. Control strategy 1 operates such that the ICE runs at a constant fuel throttle angle and the electric machine makes up the difference between the torque requested by the driver and the torque produced by the ICE. This scheme aims to minimize the amount of time that the ICE is in use by maximizing the speed at which the ICE is engaged to the wheels while maintaining the battery state of charge over the drive cycle. Control strategy 2 operates such that the ICE runs over its entire speed range and makes the ICE throttle angle a function of speed to meet the steady-state road load. The general principle behind each strategy is that the electric motor provides power for propulsion during the transients, acceleration to deceleration, and the ICE provides propulsion during cruising.

The sizes of the components for the parallel hybrid drive train are stated in Table 2.

TABLE 2
COMPONENTS OF PARALLEL HYBRID DRIVE TRAIN

ICE	1.0 liter, 32.5 kW
Motor	Vector controlled, 40 kW
Battery	Thirteen, 12-volt, lead acid

A. *Series Hybrid Electric Drive Train Design*

In a series hybrid electric vehicle, only one energy converter provides torque to the wheels while the others are used to recharge an energy accumulator, usually a battery pack. In a typical series hybrid design, an ICE/generator pair charges the batteries and only the motor actually provides propulsion. The series hybrid drive train shown in fig. 6 includes a controller and power plant and was designed based on [24]. A vector controlled induction motor powered by a D.C. battery pack of 156 volts supplies the power at the drive wheels. In addition, there is an A.P.U. (auxiliary power unit) comprising of an ICE driving an induction generator. The A.P.U. supplies power to the battery when the demanded current by the induction motor exceeds a threshold value of 75 amperes. The local controller is responsible for the following tasks

- demanding a torque (positive or negative) from the induction motor depending on drive cycle requirements.
- for switching on/off the APU.

The torque demanded from the induction motor is positive during acceleration and cruise phases of the drive cycle (motoring mode) and is negative during the deceleration phase of the drive cycle (generator mode). During the motoring mode, current is drawn from the battery (discharging) and during generation mode current is supplied to the battery (charging).

When the APU is on, the ICE is running at its optimum speed and the induction generator supplies charges the battery; in the 'off' mode, the ICE idles. Thus the APU is responsible for decreasing the drain on the battery pack, especially during the acceleration phases of the drive cycle. The ICE control is based on a "constant throttle strategy" which was found to be optimum [24].

The system control strategy for a series hybrid is not required to be as complex as the controller for a parallel hybrid since there is only one torque provider. For the series design discussed in the paper, the classic proportional, integral, and derivative (PID) controller [25] is utilized.
The sizes of the components for the series hybrid drive train are stated in Table 3.

TABLE 3
COMPONENTS OF SERIES HYBRID DRIVE TRAIN

ICE	1.2 liter, 40 kW
Motor	Vector controlled, 40 kW
Generator	Vector controlled, 40 kW
Battery	13, 12-volt, lead acid

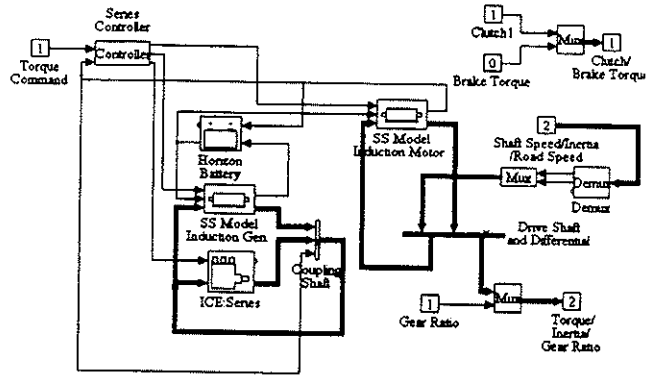

Fig. 6. Drive Train for Series hybrid vehicle

B. *Electric Drive Train Design*

In electric vehicles, all of the onboard systems are powered by batteries and electric motors. The electric drive train designed using V-Elph is shown in fig. 7.

In the electric vehicle, all the torque demanded at the drive wheels is solely met by a vector controlled induction motor powered by a D.C. battery pack of 240 volts. The controller demands a torque (positive or negative) from the induction motor, depending upon the torque demanded by the vehicle to meet the drive cycle speed. The induction motor tries to meet this demanded torque. Positive power is demanded from the induction motor (operating in motoring mode) during acceleration and cruise phases of the drive cycle and negative power is demanded during the deceleration phase of the drive cycle (operating in generator mode). During the motoring phase the induction motor draws current from the battery pack (discharging) and during the generator mode the induction motor supplies current to it (recharging) . The induction motor and battery pack are sized to satisfy the peak power requirements of the drive cycle.

The sizes of the components for the electric vehicle drive train are stated in Table 4.

TABLE 4
COMPONENTS OF ELECTRIC VEHICLE DRIVE TRAIN

Motor	Vector controlled, 40 kW
Battery	20, 12-volt, lead acid

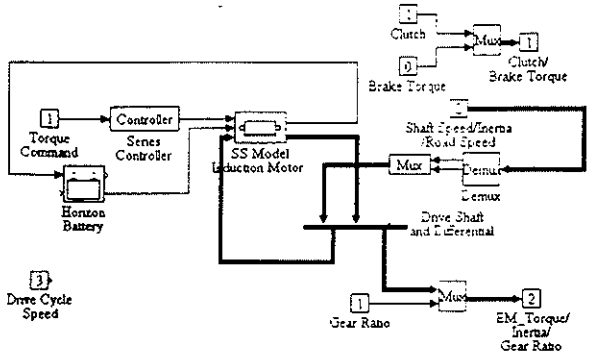

Fig. 7. Electric Vehicle Drive Train

I. SIMULATION STUDIES

Four drive cycles were applied to the various vehicle drive train designs. Drive cycle one consisted of a gradual acceleration to 120 km/h, cruise, and then a deceleration back to stop as shown in fig. 8. Drive cycles two and three were composed of the FTP-75 urban drive cycle and the federal highway drive cycle [226] as shown in figs. 9 and 10, respectively. Drive cycle four was a commuter drive cycle as shown in fig. 11 which was developed by combining three FTP-75 urban drive cycles with two federal highway drive cycles. The two highway cycles are inter-spaced between each of the urban cycles.

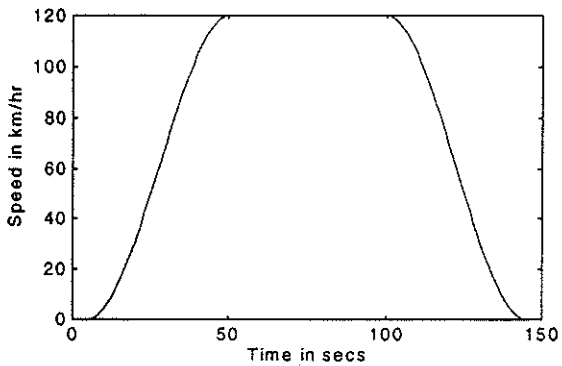

Fig. 8. Drive cycle one consisting of acceleration, cruise, and deceleration

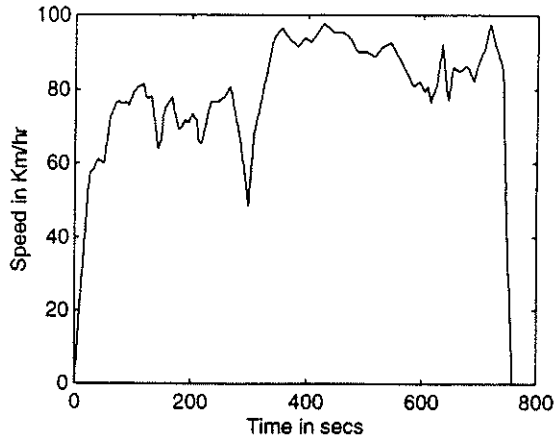

Fig. 9. FTP-75 Urban drive cycle – Drive Cycle Two

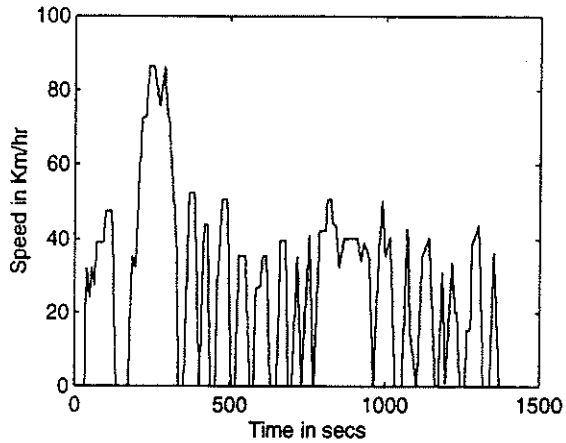

Fig. 10. Federal highway drive cycle – Drive Cycle Three

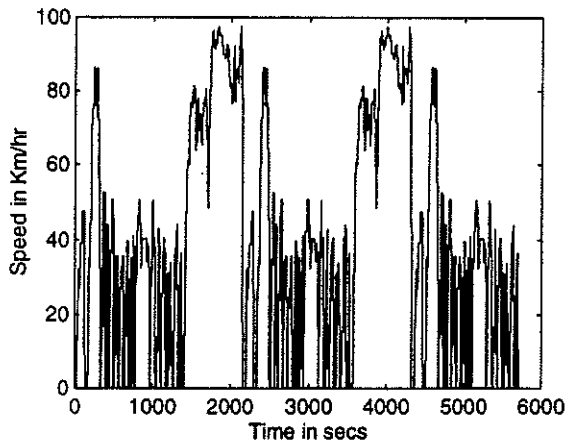

Fig. 11. Commuter drive cycle – Drive Cycle Four

The V-Elph package includes plotting tools that provide graphical displays of output variables generated during simulation studies. Also V-Elph provides a mechanism to facilitate the study of various aspects related to electric and hybrid electric vehicle drive train design such as control strategies and vehicle configurations (e.g. EV and HEV). The following figures illustrate the results of various simulation studies conducted using the four drive cycles with the five vehicle configurations.

Fig. 12 shows a plot of the electric motor (EM) torque and ICE torque versus time for the drive cycle one applied to the parallel vehicle using control strategy 1. It illustrates how the electric motor torque increases with the increase in vehicle speed. When the vehicle reaches cruising speed, the electric motor torque reduces to a slightly negative constant value while the ICE torque maintains a constant value. Then during the deceleration phase of the drive cycle, the ICE torque is at its idling torque while the electric motor torque is providing a negative torque, operating in generating mode.

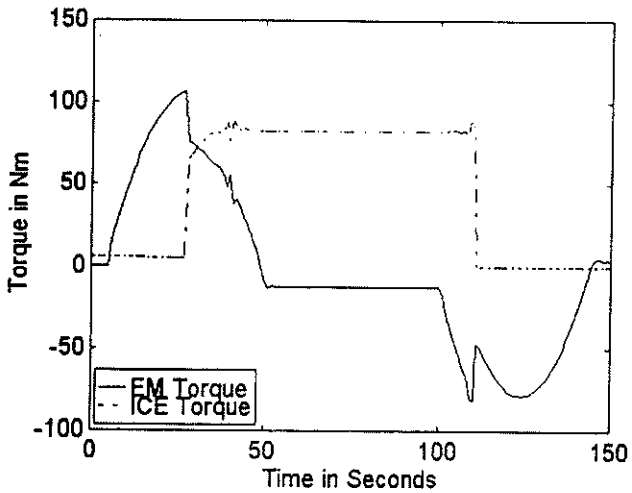

Fig. 12. EM torque and ICE torque for drive cycle one applied to the parallel vehicle with control strategy 1

Figs. 13 and 14 show the split of the ICE and electric motor torque for control strategies 1 and 2.

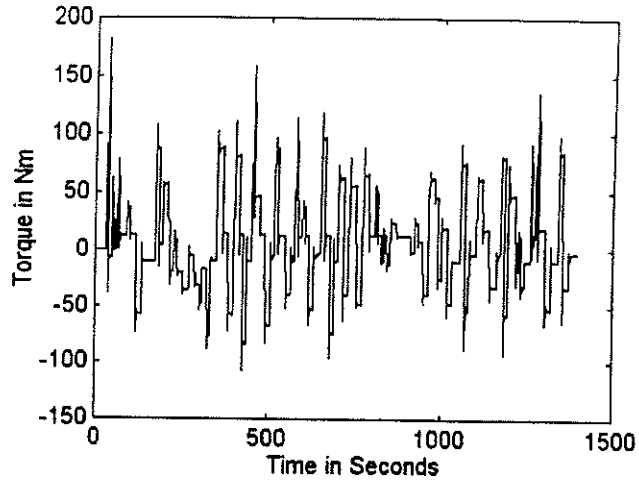

Fig. 13 (a). EM torque for federal urban drive cycle applied to parallel vehicle with control strategy 1

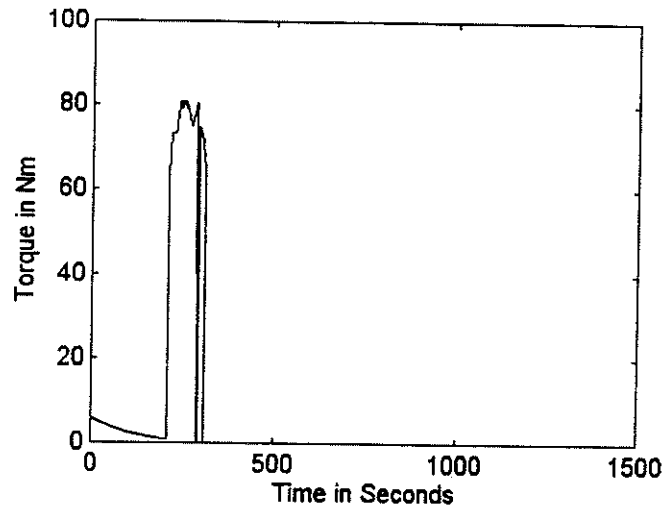

Fig. 13 (b). ICE torque for federal urban drive cycle applied to parallel vehicle with control strategy 1

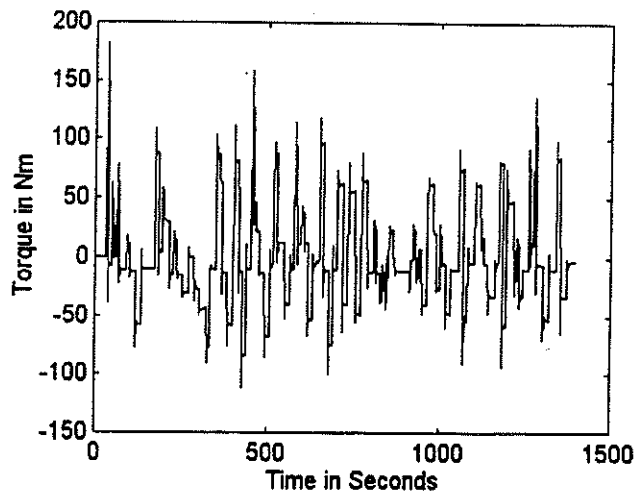

Fig. 14 (a). EM torque for federal urban drive cycle applied to parallel vehicle with control strategy 2

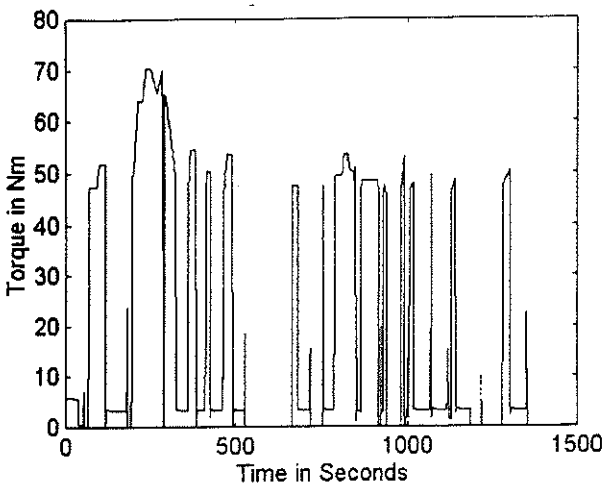

Fig. 14 (b). ICE torque for federal urban drive cycle applied to parallel vehicle with control strategy 2

Figs. 15 and 16 show the EM torque for the federal urban drive cycle applied to the series hybrid electric vehicle and electric vehicle which are virtually identical because for both vehicles the electric machine is the sole source of propulsion. In figs. 17 and 18, the differences in the battery current for the two test cases are illustrated; the battery current is larger for the electric vehicle than the series HEV.

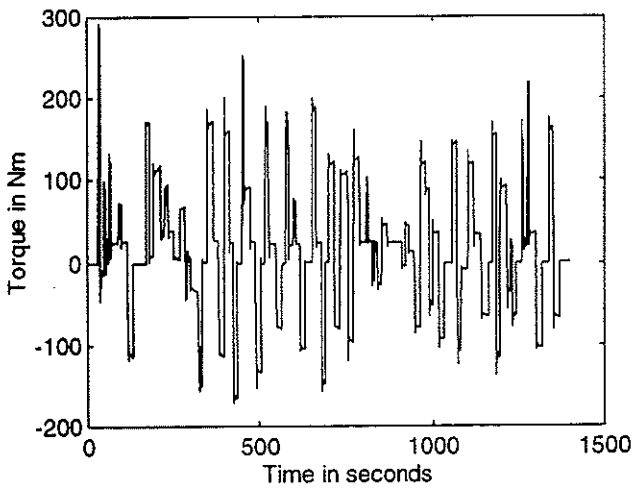

Fig. 15. EM torque for federal urban drive cycle applied to series HEV

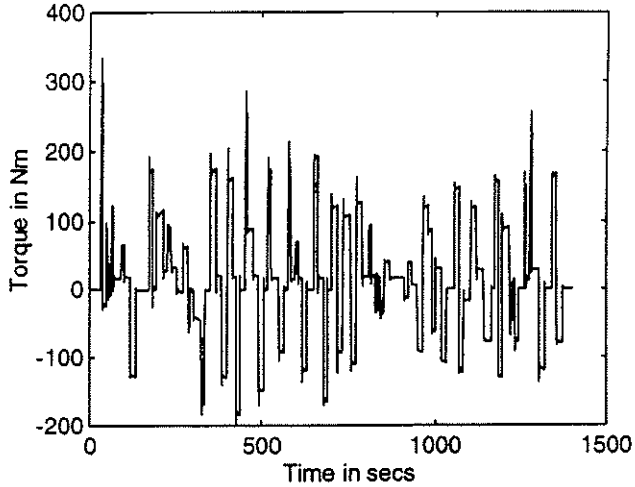

Fig. 16. EM Torque for federal urban drive cycle applied to electric vehicle

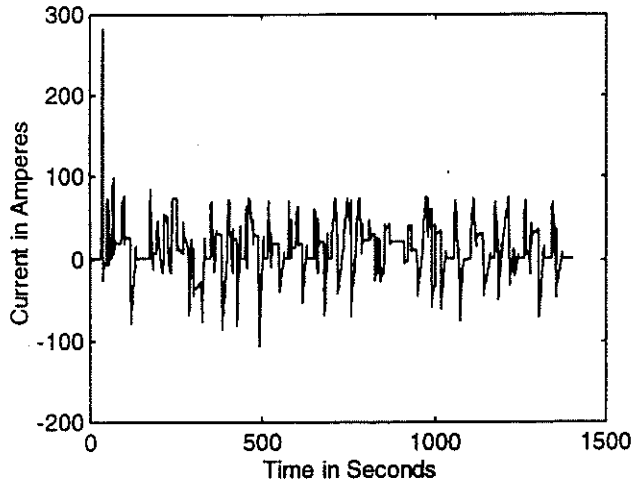

Fig. 17 Battery Current for federal urban drive cycle applied to series HEV

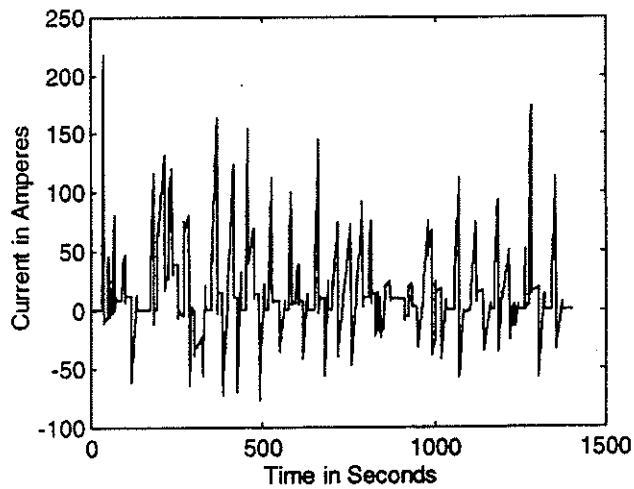

Fig. 18 Battery Current for federal urban drive cycle applied to electric vehicle

Table 5 shows a summary of results generated by the V-Elph package during the application of the four drive cycles to the five vehicle drive trains. The weight and control complexity is included in the table for each vehicle drive train. The control complexity was determined by assessing the complexity of the system controller used to manipulate the components providing propulsion to the wheels, e.g. the controller for the parallel HEV must control the ICE and electric machine. The total chemical emissions and fuel consumption of the engine and the change in the state of charge of the battery for the total drive cycle is tabulated for each vehicle.

The results for the urban drive cycle, which is composed of many quick acceleration and deceleration instances, show an improvement in the fuel consumption for the parallel HEV and series HEV. Also the engine emissions were greatly reduced. From figs. 15 and 16, it was noted earlier that the EM torque are identical for the federal urban drive cycle applied to the series HEV and electric vehicle. However, the difference in their change in the battery SoC as seen in the are due to the inclusion of the ICE in the series HEV which uses this fuel source to provide power to recharge the batteries.

The strategy of the controller for the parallel HEV using control strategy 1 was to minimize the use of the ICE. Figs. 13(a) and 13(b) shows the division of the ICE and EM torque for the urban drive cycle applied to the parallel vehicle drive train using control strategy 1. The ICE torque is only generated when the demanded vehicle speed is greater than 60 km/h. Hence the motor provides most of the power to the wheels during the drive cycle. This behavior can be seen by comparing the change in SoC for the EV of 7.58% and for the parallel HEV using control strategy 1 of 5.6% which shows that the motor in the parallel HEV is used almost as much as the motor in the EV. Also the fuel consumption (km/l) for the parallel HEV using control strategy 1 is extremely large.

Minimization of the ICE throttle is the control strategy for the parallel HEV using control strategy 2. The ICE throttle position is determined using the steady state load (aerodynamic drag and friction) required at a particular vehicle speed. In comparing the performance of this drive train using the urban and highway drive cycles, the fuel consumption, the kilometers traveled per liter, for the urban cycle is greater because the motor is used more during the urban cycle than the highway cycle.

Also the differences in the performance of the two control strategies for parallel HEV are also illustrated by the fuel consumption and change in state of charge (SoC) on the federal urban drive cycle.

Since the battery pack is the sole power supplying device in the electric vehicle, its drop in SoC is more than compared to the parallel or series hybrid vehicle.

TABLE 5 COMPARISONS BETWEEN VARIOUS VEHICLE DRIVE TRAIN CONFIGURATIONS

	Conventional	Parallel HEV control strategy 1	Parallel HEV control strategy 2	Series HEV	EV
control complexity	n/a	complex	complex	medium	simple
weight (kg)	1700	1838	1838	1908	2008
Drive Cycle One					
NOx (g/km)	2.451	1.447	1.421	2.096	NA
CO (g/km)	1.637	0.6125	0.6198	0.8544	NA
HC	0.03382	0.003336	0.00624	0.001963	NA
fuel consumption (km/l)	7.723	18.96	18.6	20.1	NA
% change in state charge	NA	+0.536	+0.3	-0.8384	-3.743
Drive Cycle Two: FTP-75 urban drive cycle					
NOx (g/km)	1.314	0.1875	0.3268	1.516	NA
CO (g/km)	1.994	0.1509	0.4926	0.6489	NA
HC	0.08234	0.01036	0.04289	0.01095	NA
fuel consumption (km/l)	5.808	56.02	21.18	19.68	NA
% change in state charge	NA	-5.6	-0.5396	-5.915	-7.58
Drive Cycle Three: Federal highway drive cycle					
NOx (g/km)	0.7071	1.04	0.86	1.574	NA
CO (g/km)	0.9732	0.7248	0.6528	0.6532	NA
HC	0.05544	0.02907	0.02962	0.002272	NA
fuel consumption (km/l)	12.4	16.5	17.23	21.89	NA
% change in state charge	NA	+10	+10.71	-9.734	-9.871
Drive Cycle Four: Commuter drive cycle					
NOx (g/km)	0.955	0.6304	0.6195	1.642	NA
CO (g/km)	1.439	0.4491	0.5907	0.6852	NA
HC	0.07379	0.01915	0.03665	0.005872	NA
fuel consumption (km/l)	6.228	24.75	18.69	20.36	NA
% change in state charge	NA	+4.2	+18.32	-34.22	-41.89

I. Conclusion

This paper discussed a new system-level modeling, simulation and analysis package developed at Texas A&M University using Matlab/Simulink to study issues related to electric vehicle (EV) and hybrid electric vehicle (HEV) design such as energy efficiency, fuel economy, and vehicle emissions. The package uses visual programming techniques, allowing the user to quickly change architectures, parameters, and to view output data graphically. It also includes detailed models of electric motors, internal combustion engines, and batteries.

The designs for four vehicle drive trains, an EV, a parallel EV, a series HEV, and a conventional ICE vehicle are presented. The results of applying a simple, a commuter, the federal urban, and the federal highway drive cycles are compared. These results illustrate the flexibility of the package for studying various issues related to electric and hybrid electric vehicle design. The simulation package can run on a PC or a Unix-based workstation.

II. Acknowledgments

Support for this work was provided by the Texas Higher Education Coordinating Board Advanced Technology Program (ATP), the Office of the Vice President for Research and Associate Provost for Graduate Studies, through the Center for Energy and Mineral Resources, Texas A&M University, and the Texas Transportation Institute.

III. References

[1] M. J. Riezenman, "Electric Vehicles," *IEEE Spectrum*, pp. 18-101, Nov. 1992.

[2] V. Wouk, "Hybrids: then and now," *IEEE Spectrum*, pp. 16-21, July 1995.

[3] A. Kalberlah, "Electric Hybrid Drive Systems for Passenger Cars and Taxis," *Tech. Rep. 910247, SAE*, 1991.

[4] B. Bates, "On the road with a Ford HEV," *IEEE Spectrum*, pp. 22-25, July 1995.

[5] M. Hayashida, and et al, "Study on Series Hybrid Electric Commuter-Car Concept," *SAE Journal SP-1243, Paper No. 970197*, Feb. 1997.

[6] A. Nikopoulos, H. Hong, and T. Krepec, "Energy Consumption Study for a Hybrid Electric Vehicle," *SAE Journal SP-1243, Paper No. 970198*, Feb. 1997.

[7] R.D. Senger, "Validation of ADVISOR as a Simulation Tool for a Series Hybrid Electric Vehicle using the Virginia Tech Future Car Lumina," Master's Thesis, Virginia Tech University, 1997.

[8] G. Cole, "Simple Electric Vehicle Simulation (SIMPLEV) v3.1," DOE Idaho National Engineering Laboratory.

[9] W.W. Marr and W.J. Walsh, "Life-cycle Cost Evaluations of Electric/Hybrid Vehicles," *Energy Conversion Management*, vol. 33:9, pp. 849-853, 1992.

[10] J.R. Bumby and et al, "Computer Modeling of the Automotive Energy Requirements for Internal Combustion Engine and Battery Electric-Powered Vehicles," *in Proceedings of IEE Pt. A*, vol. 132:5, pp. 265-79, 1985.

[11] K. B. Wipke and M. R. Cuddy, "Using an Advanced Vehicle Simulator (ADVISOR) to Guide Hybrid Vehicle Propulsion System Development," *http://www.hev.doe.gov*.

[12] D. Buntin, *Control System Design for a Parallel Hybrid Electric Vehicle*, Master's thesis, Texas A&M University, College Station, Texas, 1994.

[13] M. Ehsani, K.M. Rahman, and H.A. Toliyat, "Propulsion System Design of Electric and Hybrid Vehicles," *IEEE Transactions on Industrial Electronics*, vol. 44, Feb. 1997, pp. 19-27.

[14] H. A. Toliyat, K. M. Rahman, and M. Ehsani, "Electric Machine in Electric and Hybrid Vehicle Application," *Proceeding of ICPE ' 95*, Seoul, pp. 627-635.

[15] M. Ehsani, *Electrically Peaking Hybrid System and Method*, U.S. Patent granted in 1996.

[16] J. Howze, M. Ehsani, and D. Buntin, *Optimizing Torque Controller for a Parallel Hybrid Electric Vehicle*, U.S. Patent granted in 1996.

[17] *Proceedings of the ELPH Conference*, Texas A&M University, College Station, Texas, October 1994.

[18] K. M. Stevens, *A Versatile Computer Model for the Design and Analysis of Electric and Hybrid Drive Trains*, Master's thesis, Texas A&M University, College Station, Texas, 1994.

[19] K. L. Butler, K. M. Stevens, and M. Ehsani, "A Versatile Computer Simulation Tool for Design and Analysis of Electric and Hybrid Drive Trains," 1997 SAE Proceedings *Electric and Hybrid Vehicle Design Studies*, Book # SP 1243, Paper # 970199, pp. 19-25, February 1997, Detroit, MI.

[20] *Matlab/Simulink*, Version 4.2c.1/1.3c, The Mathworks Inc., Natick, Mass.

[21] D. Sherman, "Buick LeSabre Limited," *Motor Trend*, p. 65-73, July 1991

[22] B.K. Powell, "A Dynamic Model for Automotive Engine Control Analysis," in *Proceedings of the 18th IEEE Conference on Decision and Control*, pp. 120-126, 1979.

[23] S. Moore and M. Ehsani, "An Empirically Based Electrosource Horizon Lead-Acid Battery Model," *SAE Journal SP-1156, Paper No. 960448*, Feb. 1996.

[24] C. G. Hochgraf, M.J. Ryan, and H.L. Wiegman, "Engine Control Strategy for a Series Hybrid Electric Vehicle Incorporating Load-Leveling and Computer Controlled Energy Management," *SAE Journal SAE/SP-96/1156*, p. 11-24.

[25] G. Franklin, J. D. Powell, and M. Workman, *Digital Control of Dynamic Systems*, pp. 222-229, 1990, Addison-Wesley.

[26] U. Adler, ed., Automotive Handbook, Stuttgart, Germany: Robert Bosch GmbH, 2 ed., 1986.

Paper Number

A Study of Design Issues on Electrically Peaking Hybrid Electric Vehicles for Diverse Urban Driving Patterns

Z. Rahman, K. L. Butler and M. Ehsani
Texas A&M University

ABSTRACT

A vehicle's performance depends greatly on the operating conditions, such as journey type, driving behavior etc. Driving patterns vary with geographical location and traffic conditions. In today's global economy where automobile industries are concerned with both local and international markets, it becomes necessary to investigate vehicle performance for driving cycles of different countries and develop vehicle designs which are appropriate to the consumer's market. This paper concentrates on the issues related to designing hybrid electric vehicles. A method of optimizing the size of the principal hardware components of hybrid vehicles such as, electric motors, internal combustion engines, transmissions and energy storage devices based on the demands of different drive cycles is discussed in the paper. Driving cycles of five major countries around the globe were used for investigation: the ECE 15 used by United Nations Economic Commission for Europe (UN/ECE), the Japanese 10-15 mode, China's Beijing-11, Australian urban drive cycle and finally, the United States EPA75. The 'V-ELPH 2.01' EV-HEV computer simulation package developed at Texas A&M University was used for simulation testing.

INTRODUCTION

Hybrid electric vehicles (HEVs) are a viable alternative to conventional internal combustion engines (ICE)-based vehicles for the automobile industry due to environmental issues and exhausted petroleum resources. Recent efforts in HEV research are directed toward developing an energy efficient and cost-effective propulsion system [1,2]. But performance of automobiles depends not only on the vehicle drive train alone, but also on driving patterns such as journey type, driving behavior, etc. Moreover, while designing an HEV configuration, the constraints commonly imposed on optimizing critical component selection are: vehicle range, acceleration, maximum speed and road grades. All these factors are directly related to driving patterns. Hence, a comprehensive study on HEV performance over different driving conditions is very important for properly optimizing the key components in HEV design.

Consumer demand and driving patterns vary with geographical location and traffic conditions. For example, the rates of acceleration of the European standard driving cycles representing urban patterns of European drivers are lower than those drive cycles of United State's drivers [3]. Consumers of US demand extra ancillary loads, such as bigger air conditioners than other consumers. The impact of diverse driving conditions on vehicle performance is, in fact, delaying the introduction of Toyota's HEV model 'Prius' in US market. "Because the Prius was made for urban Japan's stop-and-go driving, the US model will most likely be completely different" - stated by Toyota's representative in Torrance [4].

The specifications required concerning HEV design may be divided into two categories. The first category is user-governed specification, which depends mostly on consumer's demand. The acceleration performance, maximum speed and fuel economy falls in this category. This category of specifications dictate the sizing of the vehicle components such as, the electric motor (EM), internal combustion engine (ICE) and transmission system. These are also the 'hardware' of HEVs. The second category is based on ecological issues such as vehicle emissions. The state or environment safekeeping organizations such as, Environmental Protection Agency (EPA) and California Air Regulatory Board (CARB) in US provide some regulations to automotive engineers concerning ICE exhausts. The EM-ICE control strategies developed by HEV designers should maintain vehicle emissions within the regulation limits. For charge-sustainable HEVs, the control mechanism should also take care of recharging the battery pack. The control strategy is the 'software' of the HEVs.

HEV design methodology may use a selective or general approach in defining vehicle specifications. In 'selective' designing the hardware specifications of HEV is optimized by selecting the minimum size of EM and ICE with a single gear transmission system to operate efficiently in a specific driving pattern. The control strategy is selected according to the requirement of the particular driving behavior. The 'general' design approach customizes the hardware and software specifications of the HEV so that it performs reasonably

well under diverse driving patterns. This approach, of course, will not give optimum result for any particular drive cycle. But it would be cost effective for automotive industries to generalize some of the design constraints, especially the hardware portion.

The concept of developing driving cycles for vehicle research technology was initially introduced to measure the fuel consumption and emissions of motor vehicles. Milkins and Watson [5] proposed other applications of drive cycles; 'evaluation of the merits of alternative vehicle design options' was one of them. In the same reference, the authors did a comprehensive statistical analysis on driving cycles of Japan, Europe, US and Australia. Later, Feng and Marc worked on analyzing driving patterns to model fuel economy of conventional ICE driven vehicles [6]. In [7], Feng and et al. presented simulation results on the impacts of driving patterns on EV and HEV performance in US conditions.

This paper focuses on the design issues of HEVs using the drive cycles of 5 major countries, i e United States, Japan, Australia, China and Europe. The drive cycles are analyzed to obtain the speed, acceleration performance and energy requirement of the vehicle. The peak power capacity of EM and ICE, and energy capacity of the battery pack is calculated for each drive cycle. The selective approach is taken to design parallel hybrid drive trains for each drive cycle. Simulation studies were done with the EV-HEV computer software package V-ELPH 2.01 [9] developed at Texas A&M University.

ELPH CONCEPT

HEV designers attempt to design a good control mechanism that will increase the fuel economy, reduce ICE emissions and accomplish charge sustainability of the energy pack of the vehicle. One of the focuses of the HEV research group of Texas A&M University is the design of parallel hybrids based on the electrically peaking hybrid (ELPH) concept [5]. In this type of control strategy the electric motor supplies the acceleration and deceleration power for the vehicle while the engine provides the average load power of the drive cycle. The main goal of this control technique is to use the ICE in the high speed region with almost smooth torque demand so that toxic emissions from the ICE is minimized and miles per gallon (mpg) fuel economy of the vehicle is optimized. Also measures to keep the state of charge (SOC) of the battery pack remaining within a specified limit during the driving period are taken into consideration. The objective of ELPH propulsion system is that the HEV should have comparable performance to conventional vehicles. The driving operation of the ELPH vehicles should also be similar to conventional vehicles.

HEV DYNAMICS

The power required to drive a vehicle depends on the following factors:

1. Rolling resistance of the tire with road
2. Aerodynamic drag
3. Inertial resistance in acceleration
4. Grade resistance
5. Transmission losses
6. Ancillary loads; i e, air conditioner, lights, stereo etc.

Since grade resistance is not included in all standard drive cycles, the effect of grade resistance in HEV design is neglected in this paper. The effect of air velocity is also eliminated from the simulations. Thus, total power demanded by the vehicle from its power plant is expressed as:

$$P = \frac{v(f_r Mg + \frac{1}{2}\rho C_d A_f v^2 + M\delta \frac{dv}{dt})}{\eta_t} + P_{aux} \quad (1)$$

where, P is vehicle power demand in watts, v is velocity of the car in m/s, f_r is coefficient of rolling resistance, M is vehicle weight in kg, g is acceleration of gravity in m/s^2, ρ is air density in kg/m^3, C_d is coefficient of air drag, A_f is frontal area of the vehicle in m^2, δ is mass factor which includes the effect of rotational inertia, η_t is transmission efficiency and P_{aux} is the power required to drive the ancillary (hotel) loads in watts.

CALCULATION OF ICE AND EM POWER FOR ELPH VEHICLES

For a conventional vehicle, all the power is supplied by the engine whereas in HEV, the driving power is supplied by the EM and the ICE. The ELPH concept mentions that the steady state portion of the driving power is provided by the ICE while the transient portion is supplied by EM. Hence, equation (1) is divided into two parts:

$$P_{ICE} = \frac{v(f_r Mg + \frac{1}{2}\rho C_d A_f v^2)}{\eta_t} + P_{aux} \quad (2)$$

$$P_{motor} = \frac{M\delta v \frac{dv}{dt}}{\eta_t} \quad (3)$$

where, P_{ICE} is the power provided by the ICE in watts and P_{motor} is the power provided by the EM in watts. The primary bottleneck considered in HEV development is the low power and energy density of the battery pack. To minimize loading on the battery pack and thus the EM, power required for auxiliary loads (P_{aux}) is considered to be delivered by the ICE. If we consider the mass and dimension for a typical vehicle model to be fixed then all the parameters except vehicle speed (v) in equation (2) and (3) becomes a constant. Hence, the engine power becomes a function of vehicle speed (v) only and motor power is proportional to the product of vehicle speed and

acceleration ($v\frac{dv}{dt}$); named as specific energy K. Therefore, the maximum engine capacity can be determined by the peak velocity (v_{max}) of the drive cycle. Similarly, the motor power rating can be determined by taking maximum specific energy (K_{max}) of the drive cycle.

CALCULATION OF BATTERY CAPACITY

The size of the battery pack is dependent on two factors. First, the battery pack should be capable of delivering motor peak power. Second, in case of charge sustainable HEVs, the battery energy should meet the requirement of keeping battery SOC within a specified limit. (For charge depleting EV/HEV, the size the of battery pack depends on the vehicle range specification). The peak power demand of the battery can be calculated by equation (3). But the energy requirement of the battery depends on the EM-ICE control strategy of HEV. Different control strategies will obtain different fuel economies and different battery energy capacities. Presently, the ELPH configuration is designed using one of two electrically peaking control strategies, referred to as control strategy 1 and control strategy 2. The descriptions of these control strategies are presented later.

In this paper, the method to determine battery energy capacity is followed from the concept [10] with an empirical model of the horizon lead-acid battery [11] developed for 'V-ELPH'. The energy supplied by the battery pack in a drive cycle at time t is:

$$E = \int_0^t P_b d\tau \qquad (4)$$

where, E is the net energy in watt-s supplied from battery pack at time t seconds and P_b in watts is the battery power. During positive motor power demand, such as acceleration and cruising, the motor power is delivered by the battery. Hence,

$$P_b = \frac{P_{motor}}{\eta_{bd}\eta_{motor}} \qquad (5)$$

where, η_{bd} is the battery discharging efficiency and η_{motor} is motor efficiency. During braking mode the motor delivers power back to the battery. But because of the chemical sluggishness involved in recharging the battery pack, the maximum regenerative braking power that the electric system can supply is limited by the maximum recharging current. Hence,

$$P_b = P_{motor}\eta_{bc}\eta_{gen} \quad , I_b \le I_{rmax} \qquad (6.a)$$

$$P_b = P_{b\,max} \quad , I_b > I_{rmax} \qquad (6.b)$$

where, η_{bc} is battery charging efficiency, η_{gen} is regenerating efficiency of EM, I_b is battery current in amperes, I_{rmax} is maximum recharging current in amperes and P_{bmax} is maximum regenerative braking power in watts. The time history of the energy delivered by the battery pack for a given drive cycle can be obtained from equations (4), (5) and (6).

For a charge sustainable HEV, the SOC of battery is always kept within a specified range. So, the battery should be capable of delivering energy with its SOC remaining within the range. Thus, the minimum energy capacity of the battery is:

$$C_b = \frac{|\Delta E_{max}|}{\Delta SOC} \qquad (7)$$

where, C_b is battery energy capacity in watt-s, ΔE_{max} is the maximum variation of battery energy in watt-s in time-energy profile, ΔSOC is the allowable range of SOC in percentage.

The equation to obtain the gear ratio between the driving units (ICE and EM) with the drive wheel is:

$$i_t = \frac{\pi n_{max} r}{30 v_{max}} \qquad (8)$$

where, i_t is the gear ratio, n_{max} is the maximum speed of ICE or EM in rpm, r is wheel radius in meters and v_{max} is maximum vehicle speed in m/s.

DRIVE CYCLES

Figure 1 presents the urban drive cycles of five countries: EPA75 of the United States, Australian urban (AU), ECE 15 of the EEC nations, M10-15 of Japan and Beijing-11 (Bj-11) of China. Drive cycles from US and Australia represent actual driving behavior while drive cycles from Europe, Japan and China were constructed by using constant accelerations and decelerations. Unusual driving conditions, such as hill climbing, load pulling, stormy weather, etc are not considered in these cycles.

ESTIMATION OF HEV HARDWARES

In this example, a typical 4 door, 5-seat family sedan was selected [10]. The vehicle specifications are:

- Weight, M — 1700kg
- Coefficient of rolling resistance, f_r — 0.013
- Coefficient of air drag, C_d — 0.29
- Frontal area, A_f — 2.13m^2
- Wheel radius, r — 0.2794m
- Ancillary load, P_{aux} — 5 kW

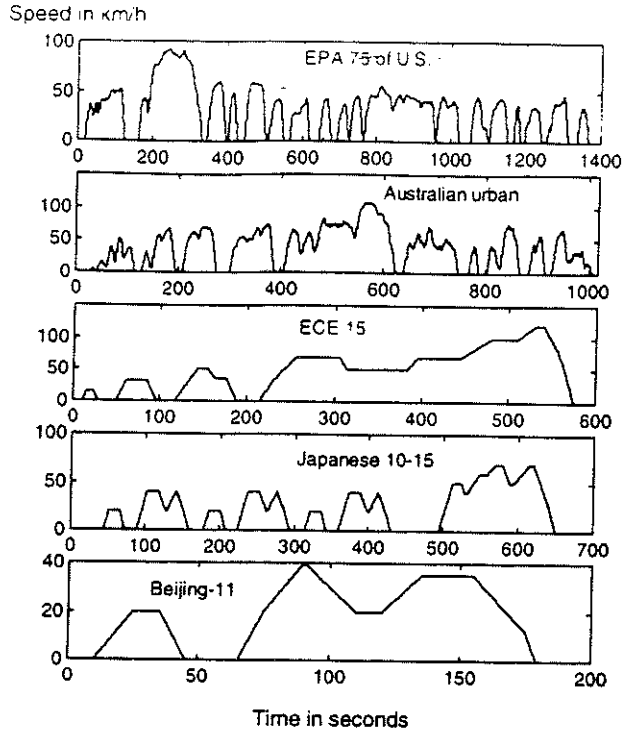

Figure 1. Velocity-time profile of the drive cycles. (See additional source section for reference).

DETERMINATION OF ICE, EM AND BATTERY POWER FOR ELPH VEHICLES

Table 1 shows the maximum speed v_{max} and maximum specific energy K_{max} of the five drive cycles. The power capacity of ICE and EM are calculated using equation (1) and (2). In the calculation, the transmission efficiency, η_t = 0.92, mass factor, δ = 1.035 and air density, ρ = 1.202kg/m^3. The peak power capacity of the battery can be calculated from equation (5) taking battery discharging efficiency, η_{bd} = 0.85 and motor efficiency, η_{motor} = 0.9.

Table 1. Determination of ICE, EM and battery power for different drive cycles.

Drive Cycles	v_{max} km/h	K_{max} m^2/s^3	P_{ICE} kW	P_{motor} kW	P_b kW
EPA 75	91.2	20	17.53	38.25	50
AU	107.5	33.5	22.8	64	82
ECE 15	120	9.5	27.8	18	23.5
M10-15	70	10.7	12.55	20.5	26.8
BJ-11	40	4	8	7.65	10

The ratings specified in table 1 show a remarkable variation of ICE and EM power for different drive cycles. Because of a very simple driving pattern, ratings obtained for BJ-11 is found to be rather impractical. So, we restrain from further investigation on BJ-11. The Australian urban cycle requires the highest power rating for EM to satisfy the high acceleration demand of the Australian drivers. On the other hand, high speed limits in European countries demand high power ICE than EM. Table 1 also shows that the variation of motor power demand is more prominent than the variation in engine power demand. Electric motors have the capability to operate in overload for a short time. Motor power, P_{motor}, specified in table 1 is basically the peak power needed by the vehicle during the very short transient period of acceleration. Usually the continuous power rating of EM is half of the peak power rating. So, a parallel HEV requires a traction motor with the power rating of 20kW continuous/ 40 kW transient to satisfy the driving performance of EPA 75. The ICE ratings shown in table 1 are, actually, the minimum power demanded by the vehicle during cruising. Road grades, stormy weather conditions, load pulling, etc were not considered in the calculation. So to factor in these conditions the rated ICE power will need to be higher than the ratings stated in table 1. Furthermore, the engine produces its peak power at a shaft speed below its maximum shaft speed (see figure 2.a). The ICE power (P_{ICE}) stated in table 1 refers to engine power at maximum car speed, which is also the maximum shaft speed. Hence, the peak ICE power must be slightly larger than P_{ICE} stated in table 1 ($P_{ICEmax} > P_{ICE}$).

DETERMINATION OF BATTERY ENERGY

Before calculating battery energy capacity, the gear ratio for the motor and engine to the drive wheels need to be calculated. Figure 2.a and 2.b show the profile for torque and power of a typical engine and motor with their shaft speeds. These figures were derived using the empirical engine model and steady state vector controlled induction motor model available in the HEV simulation software V-ELPH 2.01. In this example, the engine operating speed is taken to be 1000 rpm to 6500 rpm (figure 2.a). Motor base speed is chosen 3000 rpm with an extended operating range up to 12000 rpm (figure 2.b). The gear ratios for the engine and motor is calculated by equation (8) taking the maximum shaft speed n_{max} to be 6500 rpm for the engine and 12000 rpm for electric motor. Table 2 shows the gear ratios obtained for different drive cycles.

In this example it was considered that the engine alone is responsible to deliver power to the ancillary loads. Therefore, considering a constant 5 kW of ancillary load operating over the driving schedule the idle speed of engine is determined by the speed in which ICE is capable of delivering 5 kW of power. As engine size will vary due to different power ratings for different drive cycles, the idle speed of the engine will, therefore, be different (see table 2) for different drive cycles. A steady state motor model is used in the simulation having

braking torque 2.5 times its rated torque. The advantage of overloading the electric motor to twice its continuous power rating was not considered in the simulation. But operation above the base torque limit for 1-minute period was allowed in the simulations. The motoring and regenerating profile was considered symmetrical and efficiency of regeneration (η_{gen}) was taken as 0.85. The regenerating current (I_{max}) of the battery was limited to 100 amperes.

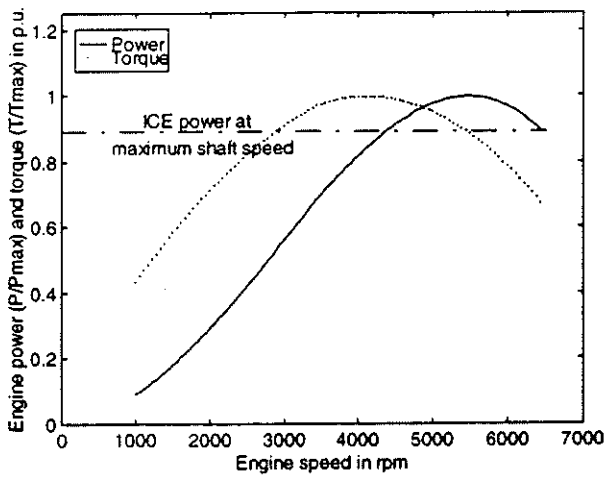

Figure 2.a Torque and power characteristics of Engine

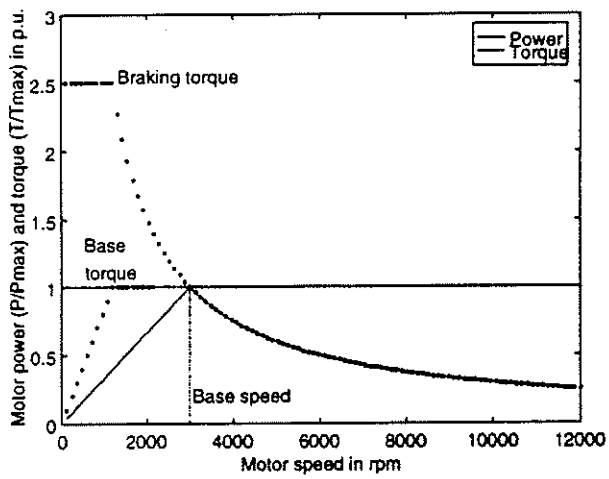

Figure 2.b Torque and power characteristics of Motor

A charge sustainable HEV requires a proper control strategy to maintain battery SOC over the driving schedule. In this example the initial SOC of battery was considered 60% and the allowable range of SOC fluctuation (ΔSOC) was taken as 20%. The two control strategies utilized in the simulations are explained below.

Control Strategy 1

Control strategy 1 (CS1) operates such that the ICE runs at a constant fuel throttle angle and the electric machine makes up the difference between the torque requested by the driver and the torque produced by the ICE. After overcoming the road load, the extra power produced by the ICE is used to charge the battery. This scheme aims to minimize the amount of time that the ICE is in use by maximizing the speed at which the ICE is engaged to the wheels while maintaining the battery state of charge of the drive cycle.

Control Strategy 2

Control strategy 2 (CS2) operates such that the ICE operates over its entire speed range and makes the ICE throttle angle a function of speed to meet the steady-state road load, as shown in figure 3. Since the battery would be depleted in a truly electrically-peaking design, the amount of power that the ICE produces needs to exceed the steady-state road load by some amount to implement a charge sustainable hybrid. In this control strategy, the gain of ICE throttle controller is varied until the battery SOC is maintained over the drive cycles.

$$\text{gain} = \frac{\text{ICE throttle command}}{\text{ICE throttle for steady state road load}} \quad (9)$$

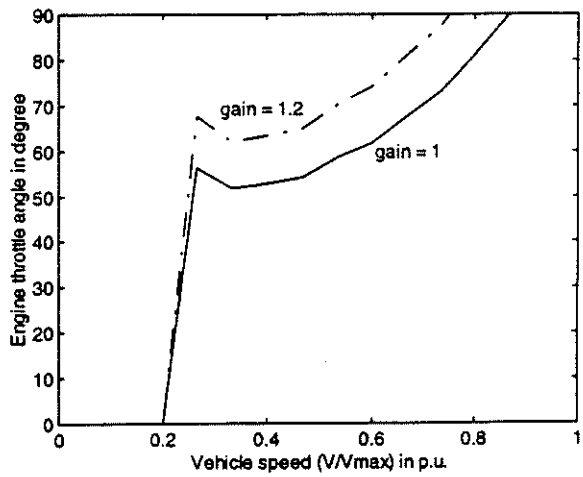

Figure 3. Variation of engine throttle angle with car speed with two different gains for control strategy 2.

The general principle behind each strategy is that the electric motor provides power for propulsion during the transients, acceleration and deceleration, and the ICE provides propulsion during cruising.

Results

Figure 4 to 7 shows the simulation results. The minimum engine and motor size corresponding to each drive cycles, as stated in table 1, was used in the simulations. Results show that the HEVs designed for each drive cycles met the driver's demand. Maximum change in battery energy is obtained from these figures. The minimum battery capacity was calculated by equation (7) taking the allowable variation in battery SOC to be 20%. A tabular presentation of the simulation results is given in table 2.

Table 2. The gear ratios and battery capacities obtained from simulation for control strategy 1 (CS1) and control strategy 2 (CS2) with four different driving cycles.

Drive Cycle	Gear ratio ICE	Gear ratio EM	ICE idle speed (rpm)	ICE engage speed for CS1 (rpm)	ICE throttle controller gain for CS2	Maximum change in battery energy (kW-hr) CS1	Maximum change in battery energy (kW-hr) CS2	Minimum battery capacity (kW-hr) CS1	Minimum battery capacity (kW-hr) CS2
EPA 75	7.51	13.86	2000	3000	1.05	0.15	0.12	0.75	0.6
AU	6.37	11.76	1500	2000	1.3	0.14	0.11	0.7	0.55
ECE 15	5.7	10.53	1500	3800	1.05	0.05	0.01	0.075	0.05
M10-15	9.78	18.06	2500	3700	1.2	0.01	0.01	0.05	0.05

The third column of table 2 shows a high ICE idle speed for the Japanese drive cycle. The reason is that the engine size for M10-15 of Japan was smaller compared to other drive cycles. To produce 5 kW of constant power for the auxiliary loads with this engine required it to operate in high speed. Frequent acceleration-deceleration in US and Australian drive cycles necessitated the ICE to be engaged with the drive wheel at a lower speed range than the European and Japanese drive cycles for CS1. High acceleration power demand of the Australian drive cycle required a throttle gain of 1.3 for CS2 to keep the change in battery energy level close to zero over the total driving period. Such a high throttle gain for the Australian driving pattern actually indicates that the engine was operating in almost wide open throttle position, which is similar to the concept of CS1. Figure 5.b, therefore, shows a very close resemblance with figure 5.a. On the other hand, driving patterns for Europe and US required a nominal throttle gain of 1.05 in CS2. The maximum variation of battery energy was less for CS2 than CS1 for all driving patterns. The reason is that in CS1 the ICE provides power in high magnitude but less frequently, whereas, in CS2 the ICE provides power in low magnitude but more frequently.

A typical 12-volt lead-acid battery cell has power density of 280 w/kg and energy density of 34 w-hr/kg. The battery energy capacity obtained in the simulation results indicates that a small size of battery pack is sufficient enough for ELPH HEVs. But the power requirement of the battery demands larger battery pack. For example, the Australian drive cycle requires a battery pack capable of producing peak power of 82 kW (= 293 kg), whereas, the energy requirement of the battery indicates a battery pack of 0.7 kW-hr (= 21kg) for CS1 and 0.55 kW-hr (= 16 kg) for CS2. The figures indicate that the battery pack needs to be sized by its peak power rating rather than the energy requirement. In fact, the acceleration performance of EV/HEVs are limited mostly because of the weight and volume of the battery pack.

In this example, transmission systems for all vehicles were considered to be single gear. A multigear transmission system will, of course, increase the acceleration performance and gradeability of the vehicle with the cost of increasing system complexity and weight.

COMPARISON STUDY

To compare the power ratings of the designed parallel HEVs for different driving conditions with a few of today's parallel HEVs manufactured by automobile industries, table 3 is presented below. The EM's peak power capacity and weight per piece of NiMH batteries used in 'Toyota Prius' was not available in [13] and hence is omitted from the table.

Table 3. ICE, EM and battery size of commercial parallel HEVs.

Manufacturer	Engine size (kW)	Motor Size Cont./Peak (kW)	Energy storage
Ford Werke AG Escort [12]	60	20/40	200 kg of NiCd, 7kWh
Subaru ElCapa [12]	48	10/19	302 kWs of capacitor + 5.7 kWh PbAcid
Toyota Prius [13]	45	30/-	40 pieces of NiMH, 55wh/kg

Comparing table 1 with table 3, it is evident that HEVs of Ford and Subaru tend to use larger engines and smaller motors compared to the ELPH based HEV designed in this paper. Using small size motors in HEV favors lower battery weight and volume. But small motors cannot produce the total accelerating power by itself. Therefore, the engine is required to operate in low speed operation, which requires multigear transmission system. The control strategies used in the three HEVs are, of course, different than the ELPH based CS1 and CS2. Yet, it is evident that Subaru's 'Elcapa' is suited more for European driving condition than the US and Australian

driving pattern. Ford's 'Escort' has ICE and EM ratings matched with US driving condition. But it might not be able to satisfy the Australian drive cycle with ELPH based strategies. The powerful engine of 'Escort' will be required to operate in acceleration modes. Toyota's 'Prius' is a truly parallel HEV with comparable ICE and EM power ratings. Of course, further studies are necessary in this area.

The engine sizes proposed for the drive cycles in table 1 are smaller than the engine size used in the vehicles of table 3. The reason is, that the five drive cycles do not include the influence of road grades, load pulling or air velocity. These factors will necessitate a larger size engine.

Drive cycles for Japan and Europe were developed with constant acceleration and deceleration. So, motor power obtained for these drive cycles show values smaller than values expected in real life. More realistic drive cycles including the effect of road grades, air velocity, load pulling will give more insight in HEV design issues.

CONCLUSION

This paper has shown the effect of diverse urban driving patterns in HEV hardware designing. Four parallel HEVs were developed for four urban areas around the globe by optimizing the size of the HEV components using ELPH concept. For conventional vehicles, resizing the engine is, more or less, the main issue as cars are imported to different driving environments. But for hybrid cars, the degrees of freedom involved in the arrangement and sizing of HEV components are so many that it becomes more complicated to design an HEV than a conventional vehicle to be compatible for different driving patterns.

This paper also emphasizes the importance of realistic and contemporary driving patterns. In this paper, the effect of the variation of auxiliary loads was not considered. But the impact of the variety of auxiliary vehicle loads on HEV performance is also another important issue as user demand will vary with geographical locations.

ACKNOWLEDGMENTS

The authors affirm their appreciation to all the students and faculty persons in the HEV research group of Texas A&M university in developing V-ELPH 2.01. Support for this work was provided by the Texas Higher Education Coordinating Board Advanced Technology Program (ATP) and the Office of the Vice President for Research and Associate Provost for Graduate Studies, through the Center for Energy and Mineral Resources, Texas A&M University.

The authors would specially like to thank Dr. Harry Watson, University of Melbourne, for providing the Australian urban drive cycle and Dr. Sado Imai, Mitsubishi motors, for providing Japan's 10 and 15 mode drive cycle.

CONTACT

K. L. Butler received the Ph.D. degree in May 1994 in electrical engineering from the Howard University where she was a NASA fellow. She received the B.S.E.E. degree in 1985 and M.S.E.E. degree in 1987 from Southern University in Baton Rouge and University of Texas in Austin, respectively. She is currently an assistant professor at Texas A&M University. She is a recent recipient of an NSF Faculty Early Career Development (CAREER) Award.

Dr. Butler was a member of technical staff at Hughes Aircraft Company from 1988-89. Her research interests are in the areas of intelligent systems, modeling and simulation, power distribution automation and system protection.

REFERENCES

1. M. Ehsani, K. M. Rahman and H. A. Toliyat, "Propulsion System Design of Electric and Hybrid Vehicles", *IEEE Trans. on Industrial Electronics, vol. 44, no. 1, Feb. 1997.*
2. A. F. Burke, "Hybrid/Electric Vehicle Design Options and Evaluations", *SAE 920447.*
3. Michel Andre' et al, "Driving Cycles for Emission Measurements Under European Conditions", *SAE 950926.*
4. D. E. Frey, "Toyota decides not to sell Prius in US this year", *http://texnews.com/1998.*
5. Milkins and Watson, "Comparison of Urban Driving Patterns", *SAE 830939.*
6. Feng An and M. Ross, "A Model of Fuel Economy and Driving Patterns", *SAE 930328.*
7. Feng An and et al, "Impacts of Diverse Driving Cycles in Electric and Hybrid Electric Vehicle Performance", *SAE 972646.*
8. M. Ehsani and et al, "Introduction to ELPH: A Parallel Hybrid Vehicle Concept", *Proceedings of the ELPH Conference, 1994.*
9. K. L. Butler, K. M. Stevens and M. Ehsani, "A Versatile Computer Simulation Tool for Design and Analysis of Electric and Hybrid Drive Trains", *SAE 970199.*
10. Y. Gao, K. M. Rahman and M. Ehsani, "The Energy Flow Management and Battery Energy Capacity Determination for the Drive Train of Electrically Peaking Hybrid Vehicle", *SAE 972647*
11. S. Moore and M. Ehsani, "An Empirically Based Electrosource Horizon Lead-Acid Battery Model", *SAE 960448.*
12. F. A. Wyczalek, "Hybrid Electric Vehicles (EVS-13 OSAKA)", *ISBN# 0-7803-3277-6, IEEE1997.*
13. "Toyota Prius", *http://www.acceleration - online.com/ toyota.htm*

ADDITIONAL SOURCES

The 'EPE 75' and 'ECE 15' drive cycles were obtained from the webpage of EPE. The 'Australian urban' was provided by Dr. Harry Watson, 'Japanese 10-15' was provided by Dr. Sado Imai. 'Beijing 11' drive cycle was reconstructed from the Ph.D. dissertation of Dr. Feng An.

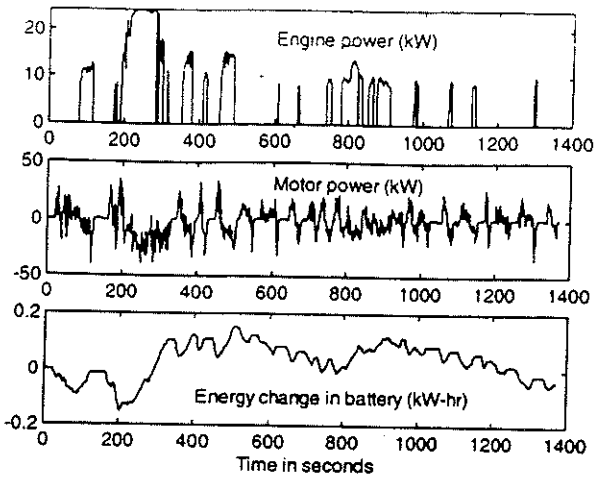

Figure 4.a Time history of engine power, motor power and energy change in battery for EPA 75 with CS1.

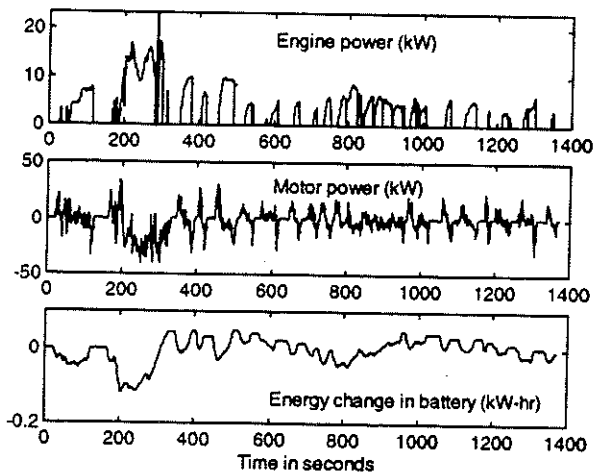

Figure 4.b Time history of engine power, motor power and energy change in battery for EPA 75 with CS2.

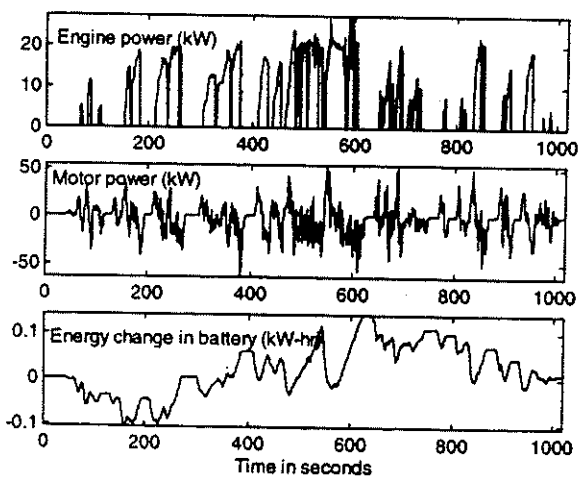

Figure 5.a Time history of engine power, motor power and energy change in battery for Australian urban with CS1.

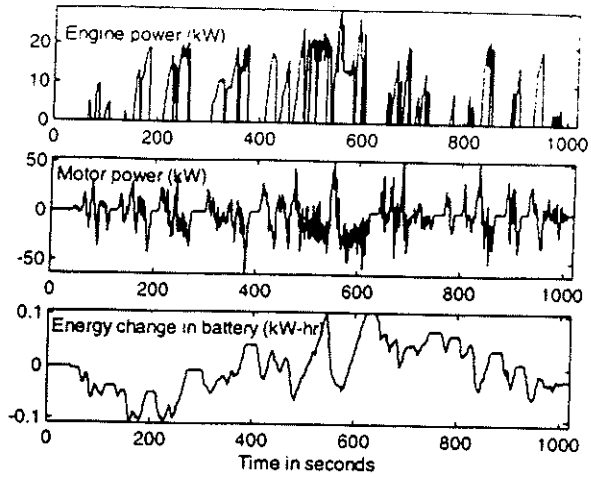

Figure 5.b Time history of engine power, motor power and energy change in battery for Australian urban with CS2.

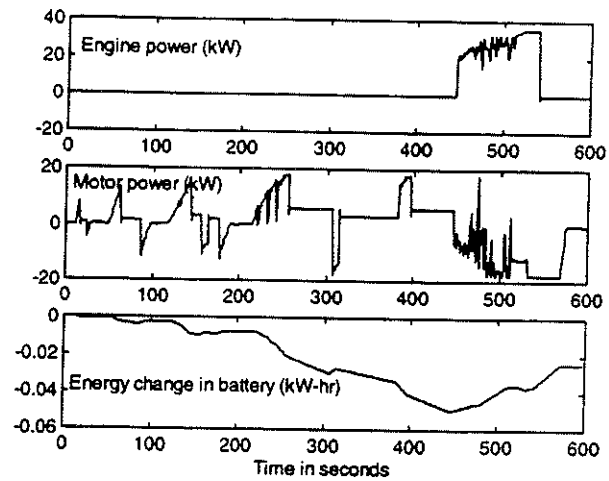

Figure 6.a Time history of engine power, motor power and energy change in battery for ECE 15 with CS1.

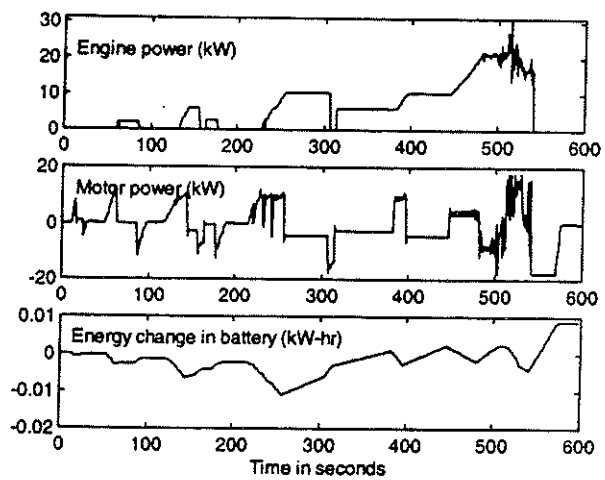

Figure 6.b Time history of engine power, motor power and energy change in battery for ECE 15 with CS2.

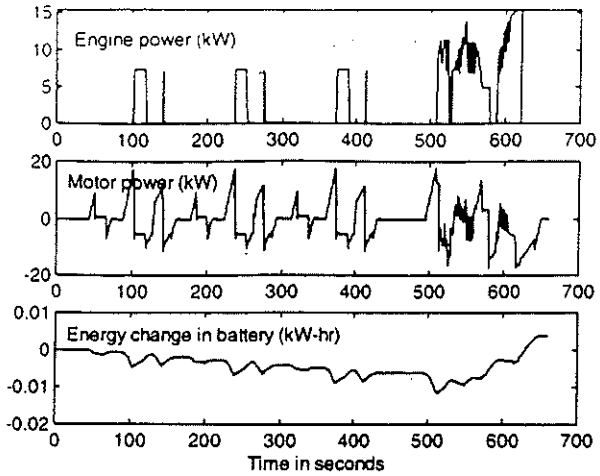

Figure 7.a Time history of engine power, motor power and energy change in battery for Japan 10-15 with CS1.

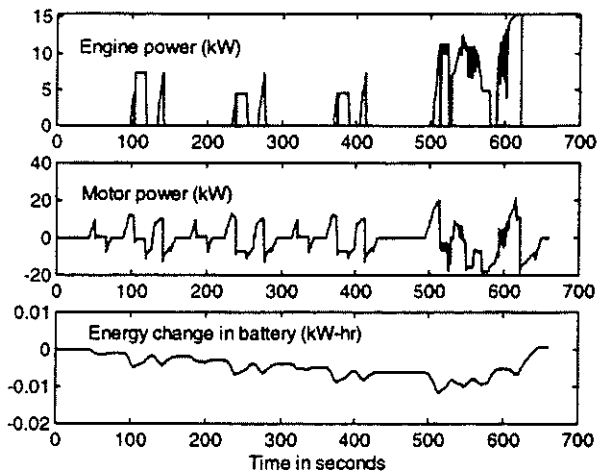

Figure 7.b Time history of engine power, motor power and energy change in battery for Japan 10-15 with CS2.